Journal of Infrastructure, Policy and Development 2025, 9(1), 10772.
https://doi.org/10.24294/jipd10772

Article

Visualization microclimate scenarios of Classical Chinese Garden in Suzhou, China

Tang Jiadai[1,2], **Wan Yusryzal Bin Wan Ibrahim**[1,*]

[1] Faculty of Built Environment and Surveying, Universiti Teknologi Malaysia, Johor Bahru 81310, Malaysia
[2] Infrastructure Department & Office of New Campus Construction, Jiangsu University of Technology, Changzhou 213001, China
*** Corresponding author:** Wan Yusryzal Bin Wan Ibrahim, wyusryzal@utm.my

CITATION

Jiadai T, Ibrahim WYBW. (2025). Visualization microclimate scenarios of Classical Chinese Garden in Suzhou, China. Journal of Infrastructure, Policy and Development. 9(1): 10772. https://doi.org/10.24294/jipd10772

ARTICLE INFO

Received: 4 December 2024
Accepted: 27 December 2024
Available online: 13 January 2025

Abstract: The intensification of urbanization worldwide, particularly in China, has led to significant challenges in maintaining sustainable urban environments, primarily due to the Urban Heat Island (UHI) effect. This effect exacerbates urban thermal stress, leading to increased energy consumption, poor air quality, and heightened health risks. In response, urban green spaces are recognized for their role in ameliorating urban heat and enhancing environmental resilience. This paper has studied the microclimate regulation effects of three representative classical gardens in Suzhou—the Humble Administrator’s Garden, the Lingering Garden and the Canglang Pavilion. It aims to explore the specific impacts of water bodies, vegetation and architectural features on the air temperature and relative humidity within the gardens. With the help of Geographic Information System (GIS) technology and the Inverse Distance Weighted (IDW) spatial interpolation method, this study has analyzed the microclimate regulation mechanisms in the designs of these traditional gardens. The results show that water bodies and lush vegetation have significant effects on reducing temperature and increasing humidity, while the architectural structures and rocks have affected the distribution and retention of heat to some extent. These findings not only enrich our understanding of the role of the design principles of classical gardens in climate adaptability but also provide important theoretical basis and practical guidance for the design of modern urban parks and the planning of sustainable urban environments. In addition, the study highlights GIS-based spatial interpolation as a valuable tool for visualizing and optimizing thermal comfort in urban landscapes, providing insights for developing resilient urban green spaces.

Keywords: visualization microclimate; Classical Chinese Gardens (CCGs); Geographic Information System (GIS); Inverse Distance Weighting (IDW)

1. Introduction

The world is experiencing an unprecedented pace of urbanization. According to recent data, over half of the global population resides in urban areas, a figure projected to reach nearly 70% by 2050 (United Nations, 2018). This rapid urbanization brings profound changes to land use, urban form, and the built environment, contributing to significant alterations in local and global climates (Henderson and Turner, 2020; Sun et al., 2020). By 2017, urban regions housed more than 4.3 billion people. Urbanization has been especially pronounced in China, with the urbanization rate increasing from 10% in 1949 to over 64.7% by 2020. Projections suggest that this trend will continue, with China’s urban population expected to rise by approximately 200 million by 2030, reaching an urbanization rate of 70% (National Bureau of Statistics, 2018).

However, rapid urbanization presents significant challenges, particularly with respect to the urban thermal environment. The process of urban expansion alters natural landscapes, replacing vegetated areas with impervious surfaces such as asphalt and concrete, which absorb and retain heat. This transformation intensifies the Urban Heat Island (UHI) effect, a phenomenon where urban areas experience higher temperatures than their rural surroundings. The UHI effect exacerbates climate warming, contributing to increased energy consumption, deteriorated air quality, and heightened risks of heat-related illnesses and mortality (Peng et al., 2019; Santamouris, 2015). According to the Intergovernmental Panel on Climate Change (IPCC), global surface temperatures have already risen by approximately 1.1 ℃ since the pre-industrial period, with further warming projected to exceed 1.5 ℃ by 2050 under current emission trajectories (IPCC, 2021).

In this context, the importance of sustainable urban design and climate adaptation strategies cannot be overstated. Among the various strategies, urban green spaces, including parks and gardens, play a crucial role in mitigating the adverse effects of urbanization on the thermal environment. By providing shade, evapotranspiration, and improved air circulation, urban green spaces can reduce ambient temperatures, enhance thermal comfort, and alleviate UHI effects (Ren et al., 2022). Specifically, the design and spatial configuration of these green spaces have a profound impact on their cooling performance. Recent studies have highlighted the shift in focus from large urban parks to smaller-scale green spaces and even microclimates within urban environments, emphasizing the need for localized climate interventions (Nazarian et al., 2017; Yu et al., 2020).

In China, the historical tradition of Classical Chinese Gardens (CCGs) offers a rich repository of climate-sensitive landscape design principles. Characterized by intricate spatial layouts and the harmonious integration of natural elements such as water bodies, vegetation, and rocks, these gardens exemplify passive climate control strategies. For centuries, CCGs have been admired for their capacity to modulate temperature and humidity, creating cool, comfortable microclimates even during the summer heat (Guo et al., 2022; Xiong et al., 2020). Scholars have noted the efficacy of traditional garden designs for climate adaptation. For example, Yang Hongxun, in "Theory of Jiangnan Gardens," posits that features such as building orientation, plant placement, and water surfaces enhance light exposure, aesthetics, and climatic improvement. Similarly, Deng Qisheng, in "Garden and Environmental Protection," emphasizes the role of traditional gardens in enhancing building microclimates. More recently, CCGs have been recognized as models of effective microclimate design, utilizing centuries of observation and adaptation. These gardens employ various landscape elements to create favorable thermal conditions, demonstrating the potential for incorporating traditional designs into contemporary urban planning. The spatial arrangement of environmental factors, including air temperature, humidity, and physiological equivalent temperature, is highly influenced by the layout of these elements, underscoring the importance of integrating landscape design with local climate conditions (Guo et al., 2022). Research by Jin and Xiong (2017) explored specific techniques for improving microclimates within CCGs during winter, showing that these gardens are capable of creating suitable environments year-round (Yan et al., 2018; Zhou, 2014). Therefore, preserving and incorporating traditional Chinese garden design principles is essential for maintaining cultural heritage while fostering sustainable urban landscape development.

As the research process advances, visualization techniques have become increasingly prominent. Geographic Information System (GIS) technology offers a powerful and widely adopted tool for evaluating the potential impacts of climate change on urban populations and infrastructure (Back et al., 2022). GIS facilitates the visualization and analysis of spatial relationships and patterns by integrating database operations, statistical analyses, and geographic mapping. For example, open-source GIS tools allow for microclimate monitoring and simulation, offering strategies to mitigate urban thermal anomalies (Guerri et al., 2023). Through remote sensing, GIS can evaluate thermal responses in urban areas with varying built densities (Mangiameli et al., 2022). Moreover, GIS-based modeling approaches can enhance existing microclimatic models, improving assessments of human thermal comfort in urban settings. Inverse Distance Weighting (IDW), a commonly employed interpolation technique, offers a weighted average approach to interpolate values across a spatial field based on proximity to sample points, which is particularly effective for estimating unknown points (Huang et al., 2011). This method prioritizes nearby data points, enhancing the accuracy of predictions related to microclimatic conditions, especially in complex environments like CCGs (Nusret and Dug, 2012).

Thus, this study aims to investigate the microclimatic scenarios within CCGs, focusing on the interactions between water bodies, vegetation, grass, and architectural structures. By examining three prominent CCGs in Suzhou—Humble Administrator's Garden, Lingering Garden, and Canglang Pavilion. The three classical gardens, The Humble Administrator's Garden, Lingering Garden and Canglang Pavilion, were chosen based on their historical significance, iconic status and representation of traditional Chinese garden architecture. Each garden embodies design principles that have been passed down for centuries, harmonizing natural elements such as water bodies, vegetation and rocks to create passive climate regulation strategies. The Humble Administrator's Garden, built in the Ming Dynasty, is the largest and most famous classical garden in Suzhou, with its vast water features, pavilions, bridges and waterways, and winding paths. The Lingering Garden, with its distinctive landscape elements, demonstrates the interplay of vegetation, water bodies, and architectural structures in regulating thermal conditions. Meanwhile, the Canglang Pavilion is the oldest of the three gardens, and its simple and harmonious layout reflects the Taoist philosophy of becoming one with nature. These gardens not only preserve cultural heritage, but also demonstrate the potential for integrating traditional design into contemporary urban planning, and are exemplary representatives of their kind. This research seeks to assess the efficacy of traditional landscape designs in reducing urban thermal stress. The article quantifies the specific effects of landscape elements on air temperature and relative humidity through spatial interpolation and other methods, providing empirical support for landscape microclimate research. In addition, it explores the potential of applying traditional landscape design principles in modern urban environments, enriching the theoretical system of urban green space planning and design. These theoretical explorations not only help to deepen our understanding of the relationship between landscape and microclimate, but also provide new perspectives and ideas for future research on sustainable urban development. The findings aim to advance knowledge on sustainable urban design, informing future efforts to develop thermally comfortable, resilient urban landscapes.

2. Study area

This study focuses on three Classical Chinese Gardens (CCGs) located in Suzhou, Jiangsu Province, China: The Humble Administrator’s Garden, Lingering Garden, and Canglang Pavilion. Suzhou, situated in eastern China (31°18′00″ N, 120°37′10″ E), lies on the lower reaches of the Yangtze River and the shores of Lake Tai (Taihu), one of China’s largest freshwater lakes (**Figure 1**). Covering approximately 8488 square kilometers (3277 square miles), Suzhou experiences a subtropical monsoon climate characterized by four distinct seasons, with hot, humid summers and cool winters. According to data from the Suzhou Meteorological Bureau, the temperature in Suzhou typically varies from 3.7 ℃ to 32.1 ℃ annually, with the hottest season spanning June to September and an average daily high above 28.3 ℃. July is typically the hottest month, with an average high of 32.78 ℃, posing risks to public health, increasing energy demand, and potentially impacting the quality of urban life. As such, the city provides an ideal setting for examining the potential of landscape design to mitigate urban heat through traditional garden elements.

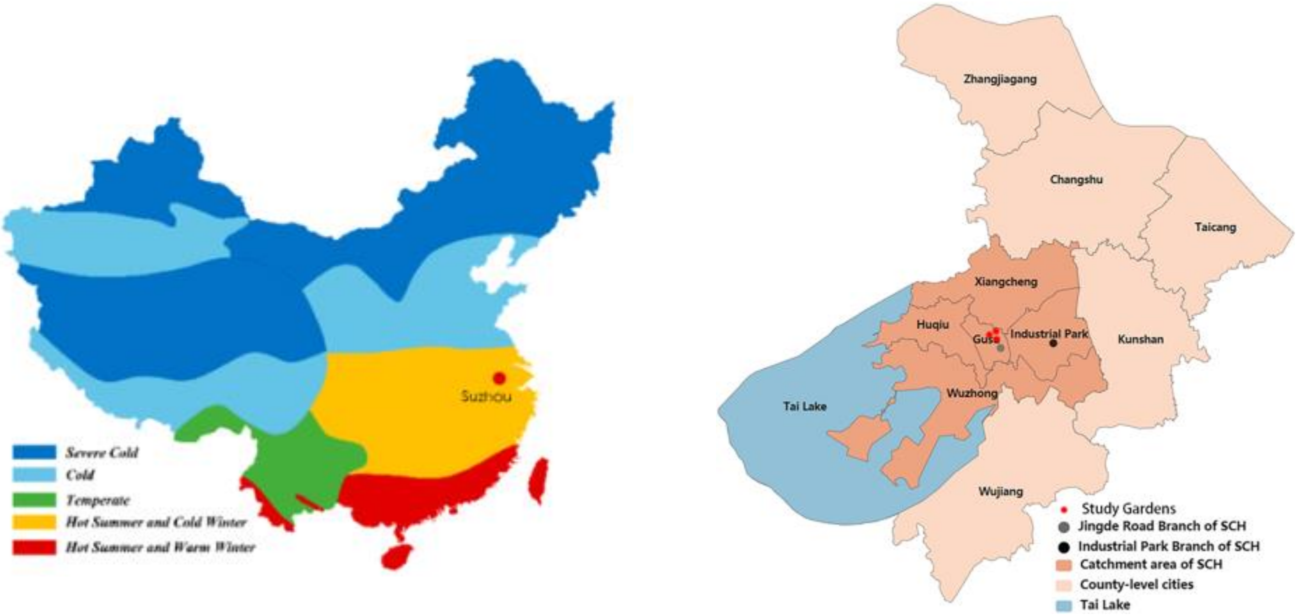

(a) Location of Suzhou in China. **(b)** Location of study areas in Suzhou.

Figure 1. Location of study area.

Each of the selected gardens represents a pinnacle of traditional Chinese landscape architecture and serves as a case study for exploring the interaction between landscape design and microclimatic regulation. The Humble Administrator’s Garden, constructed during the Ming Dynasty in 1509, is the largest and most renowned classical garden in Suzhou, encompassing approximately 5.2 hectares (**Figure 2**). Its design integrates vast water features, which occupy nearly one-third of its total area, with interspersed pavilions, bridges, and winding pathways. The garden’s layout embodies the principle of “borrowing scenery” by incorporating views of the surrounding natural and built environments seamlessly (Chen and Li, 2020). The combination of water and dense vegetation creates a cool, humid microclimate, providing thermal comfort even during summer's peak temperatures (Zhou et al., 2021).

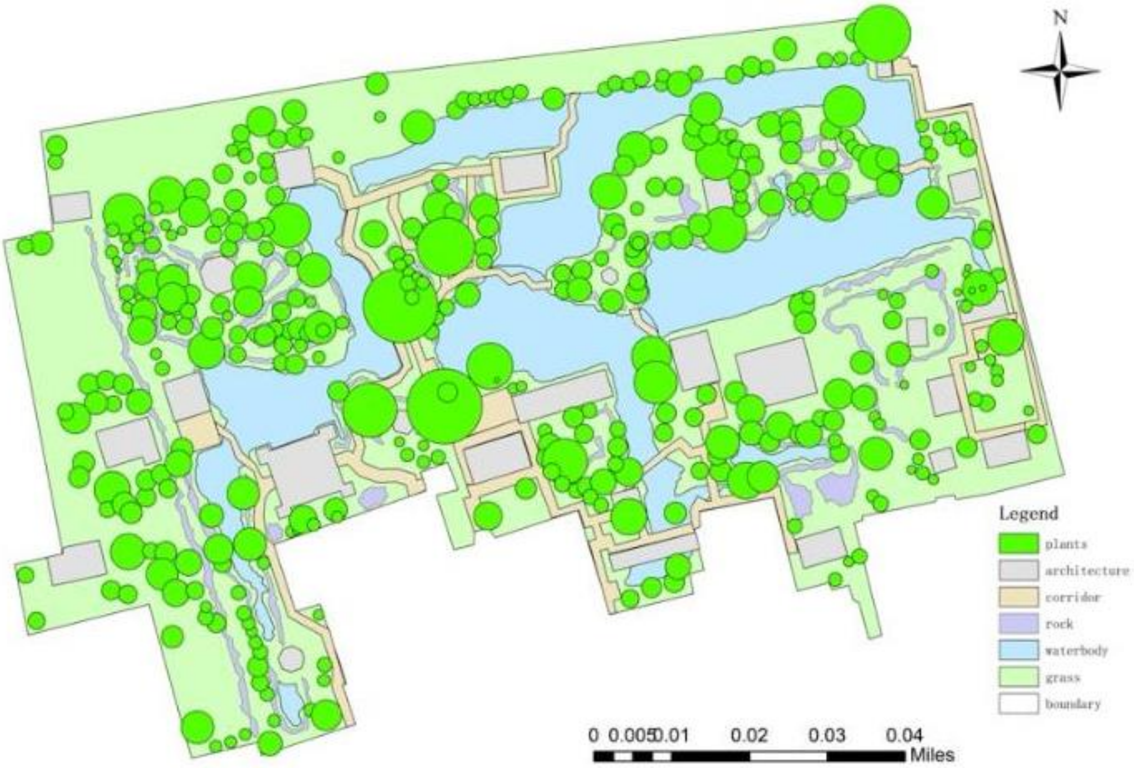

Figure 2. Plan of the Humble Administrator's Garden.

The Lingering Garden, established in 1593, is renowned for its intricate stonework and architectural elegance, spanning 2.3 hectares (**Figure 3**). A central pond, numerous rockeries, and diverse plant species contribute to its aesthetic and ecological richness. The garden's design emphasizes spatial sequence and fluid transitions between indoor and outdoor spaces, facilitating a dynamic interplay of light, shadow, and airflow (Wang and Zhang, 2019). This compact, harmonious design enables the garden to offer a cooling effect and serve as an optimal study site for understanding microclimate regulation within smaller urban green spaces (Liu et al., 2020).

The Canglang Pavilion, constructed during the Northern Song Dynasty in 1044, is the oldest of the three gardens and occupies 1.6 hectares (**Figure 4**). Its layout emphasizes simplicity and harmony with nature, reflecting the Daoist philosophy of blending with the natural world. The pavilion overlooks a central pond and is surrounded by dense vegetation and rocky outcrops, with pathways and pavilions creating shaded, cooling areas. Despite its relatively modest size, the Canglang Pavilion demonstrates efficient microclimatic performance, with strategically placed water and vegetation elements that promote thermal comfort and improve air circulation (Fang and Chen, 2019).

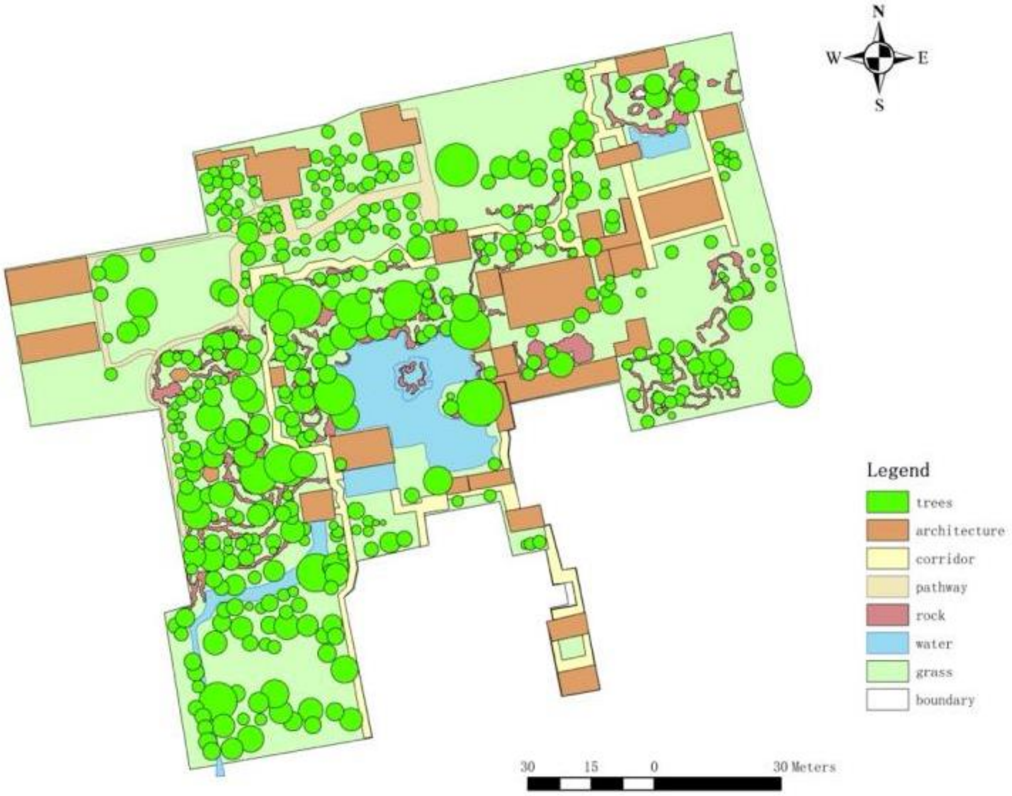

Figure 3. Plan of the Lingering Garden.

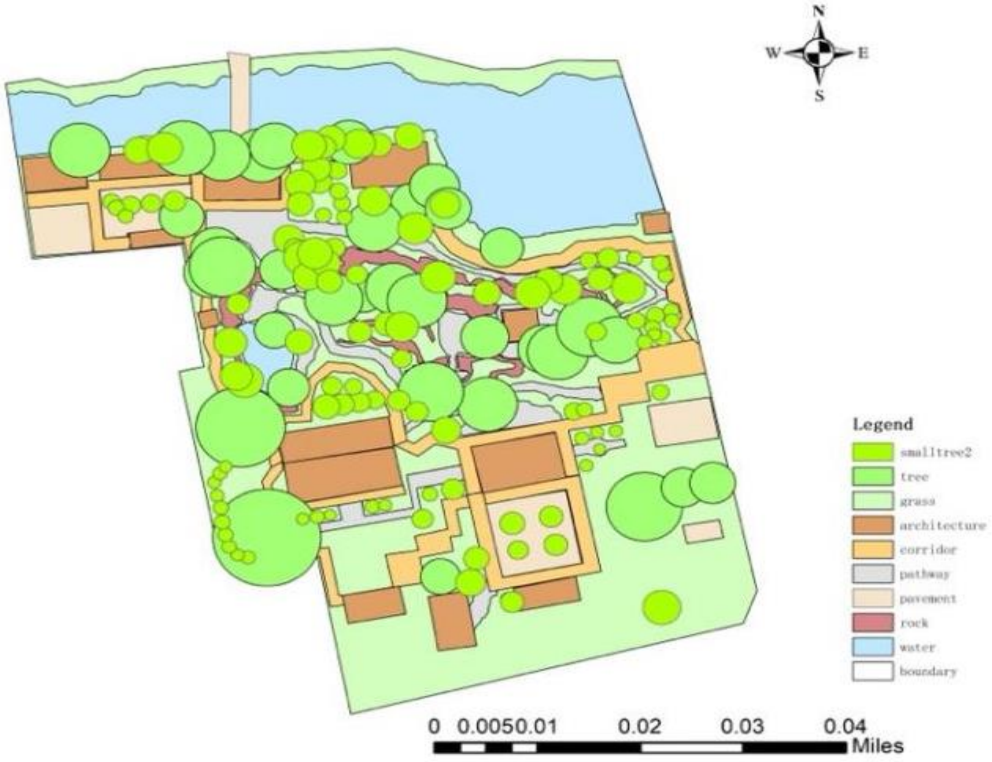

Figure 4. Plan of the Canglang Pavilion.

3. Methodology

The study follows a multi-stage methodology, beginning with defining the study area boundaries and obtaining relevant spatial data. The subsequent stages involve conducting a microclimatic survey, developing a GIS database, performing spatial interpolation analysis, and finally, interpreting the results to understand the microclimatic performance of each garden in relation to thermal comfort.

3.1. Field measurements

A sequence of measurements was implemented to collect the climate data of three CCGs. First, climatic stations were labeled in the park as the climatic data collection stations according to the surrounding landscape elements, plant amounts, and built-up features (**Figure 5**). During the period of July to August, which is often characterized by hot summer weather in Suzhou, data on weather conditions and human behavior are gathered for a duration of 22 days, specifically from 20 July to 10 August. The Delixi digital anemometer DECEMDAH30 and Delixi thermometer DECEMTMC1380 measure air temperature, wind velocity, surface temperature, and surface temperature. Simultaneously, human observation is documented when individuals are present for a duration exceeding 10 minutes. The objective of extending the duration beyond 10 minutes is to gather the individuals' preferences over the summer.

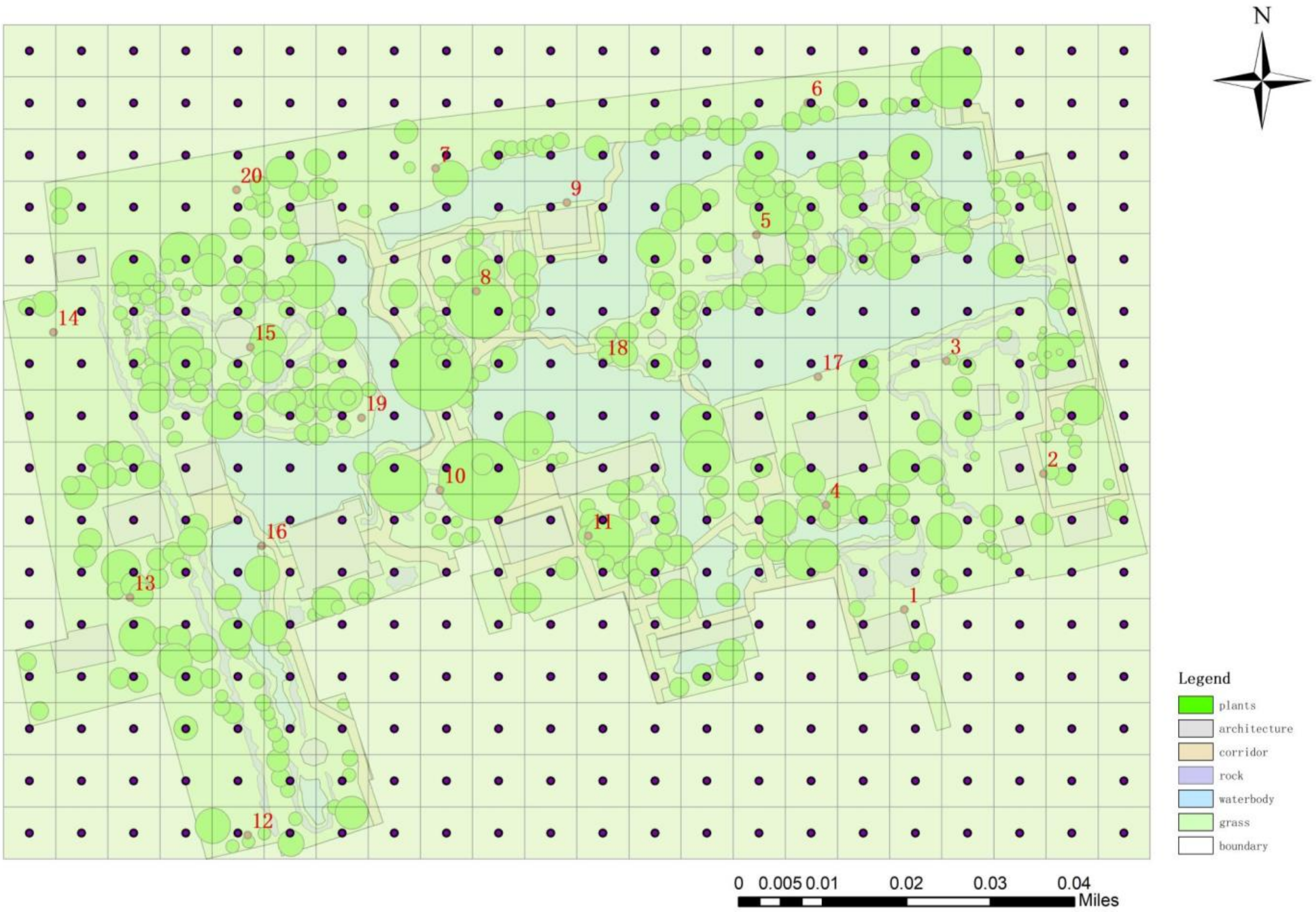

(a) Humble Administrator's Garden.

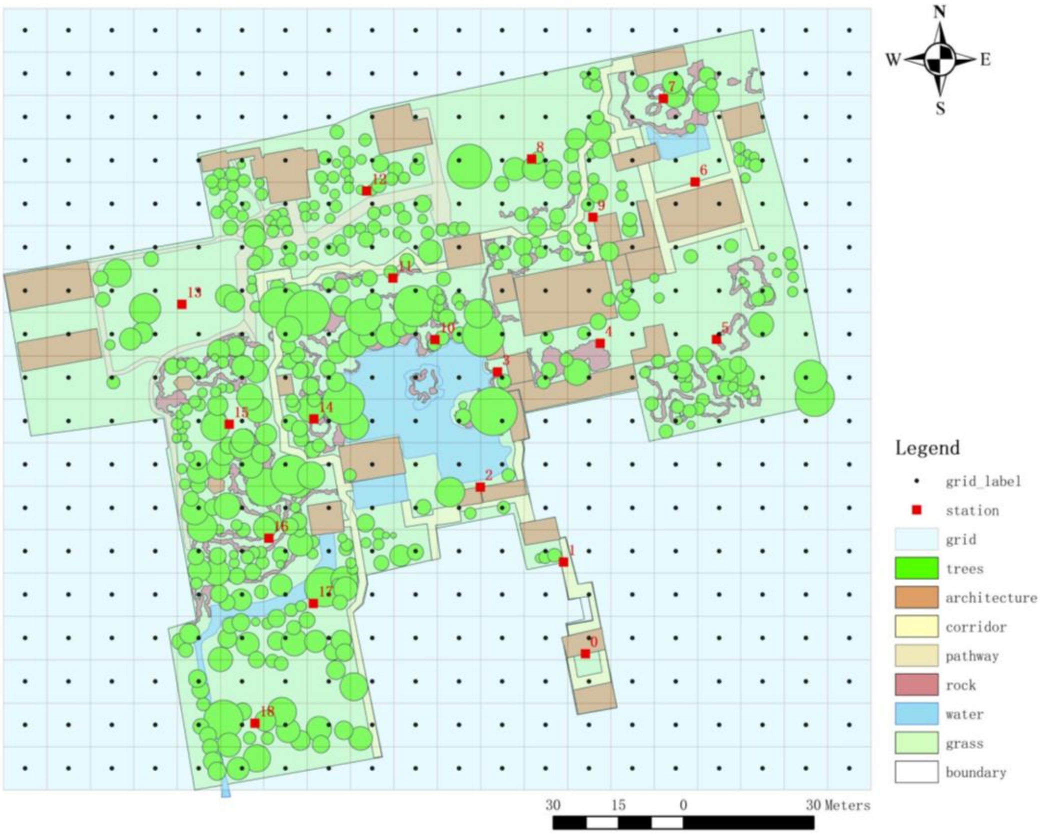

(b) Lingering Garden.

(c) Canglang Pavilion.

Figure 5. Climate station of each garden.

3.2. Development of the GIS database

The ArcGIS software is used for data management and processing. The GIS database includes five stages. Firstly, the base map was prepared, and the aerial photo was derived from Google Maps. The coordinate system was set up as CGCS2000_3-Degree_GK_CM_120E, and all the data are referred to the coordinate system. Secondly, the landscape features of three CCGs were digitized in each layer, including water bodies, plants, and buildings. Thirdly, several points were digitized for microclimate stations as input layers to record the climatic data. The data type for the attribute was identified and developed for the necessary column. Finally, the collected information, including air temperature, relative humidity, wind velocity, and surface temperature, was imported and managed in the attribute table.

3.3. Spatial interpolation analysis

IDW is the main interpolation tool in the study. The value at known sites is used to estimate a variable's value at new locations. The fundamental principle involves a weighted linear combination of sample points and relies on both statistical and mathematical approaches to generate surfaces and compute the predictions for unmeasured points. The IDW is calculated using the following equation:

$$\hat{Z}\,(x_0) = \sum_{i=1}^{n} z\,(x_i) \cdot {d_{ij}}^{-p} / \sum_{i=1}^{n} {d_{ij}}^{-p}$$

Z is the interpolated value of a grid node, X_i is the neighboring data points, and d_{ij} is the distance between the grid node and data points. The spatial interpolation then interpolates the whole scenario of microclimate at the study area for the air temperature and humidity. In this study, we also analyzed the factor weights using the IDW method to determine the relative importance of different landscape elements on microclimate impacts.

4. Results

4.1. Impact of landscape elements on air temperature

The analysis of air temperature within the Humble Administrator's Garden reveals a clear correlation between surface temperature patterns and spatial configurations of landscape elements (**Figure 6**). Temperature recordings generally increased from morning through midday, peaking around 13:30, with maximum air temperatures at stations 0, 1, and 17, where values exceeded 37 ℃. In the morning, air temperatures were notably lower in areas proximate to water bodies and shaded by dense vegetation. Stations 12 and 14, which benefit from both water and vegetation, displayed reduced temperatures during the early hours, underscoring the cooling influence of these elements. Midday measurements indicated significant temperature rises, particularly in exposed, sunlit areas and near rockeries. The highest temperatures during this period were recorded at stations 2, 17, and 18, suggesting that solar radiation and the thermal mass of rockeries contribute to localized heating. As afternoon transitioned to evening, air temperatures gradually decreased, with the cooling effect more pronounced in vegetated and shaded areas. Water bodies in particular helped sustain moderate air temperatures, impeding rapid declines in thermal readings. Notably, stations like 12 and 16 near water features exhibited relatively stable temperature profiles throughout the day.

In the Lingering Garden, temperature variations were closely tied to the garden's unique landscape elements (**Figure 7**). Vegetation and water bodies functioned as natural coolers, whereas rockeries and architectural structures tended to retain and radiate heat. In the early morning (7:30 to 9:30), the southwest corner, rich in dense vegetation, recorded cooler temperatures due to moisture retention from the night and shading effects, creating a more comfortable microclimate. Conversely, the northwest corner, with sparse vegetation, displayed relatively higher temperatures due to increased exposure to sunlight. Midday recordings (11:30 to 15:30) indicated significant temperature increases, especially in areas with minimal vegetation cover and direct sun exposure. Stations 0 and 1 recorded the highest temperatures, attributed to the lack of shading and prolonged solar exposure. Additionally, architectural pathways and rockeries contributed to heat retention. As the day progressed, temperatures started to decline, but the rate of cooling varied by landscape type. Stations with substantial vegetation, such as 16 and 18, maintained cooler temperatures due to evaporative cooling. In contrast, hardscape elements like rocks and paved paths, as seen in stations 0 and 13, released stored heat more slowly, sustaining higher temperatures into the evening. This differential cooling indicates the interplay of landscape elements in modulating thermal conditions within the garden.

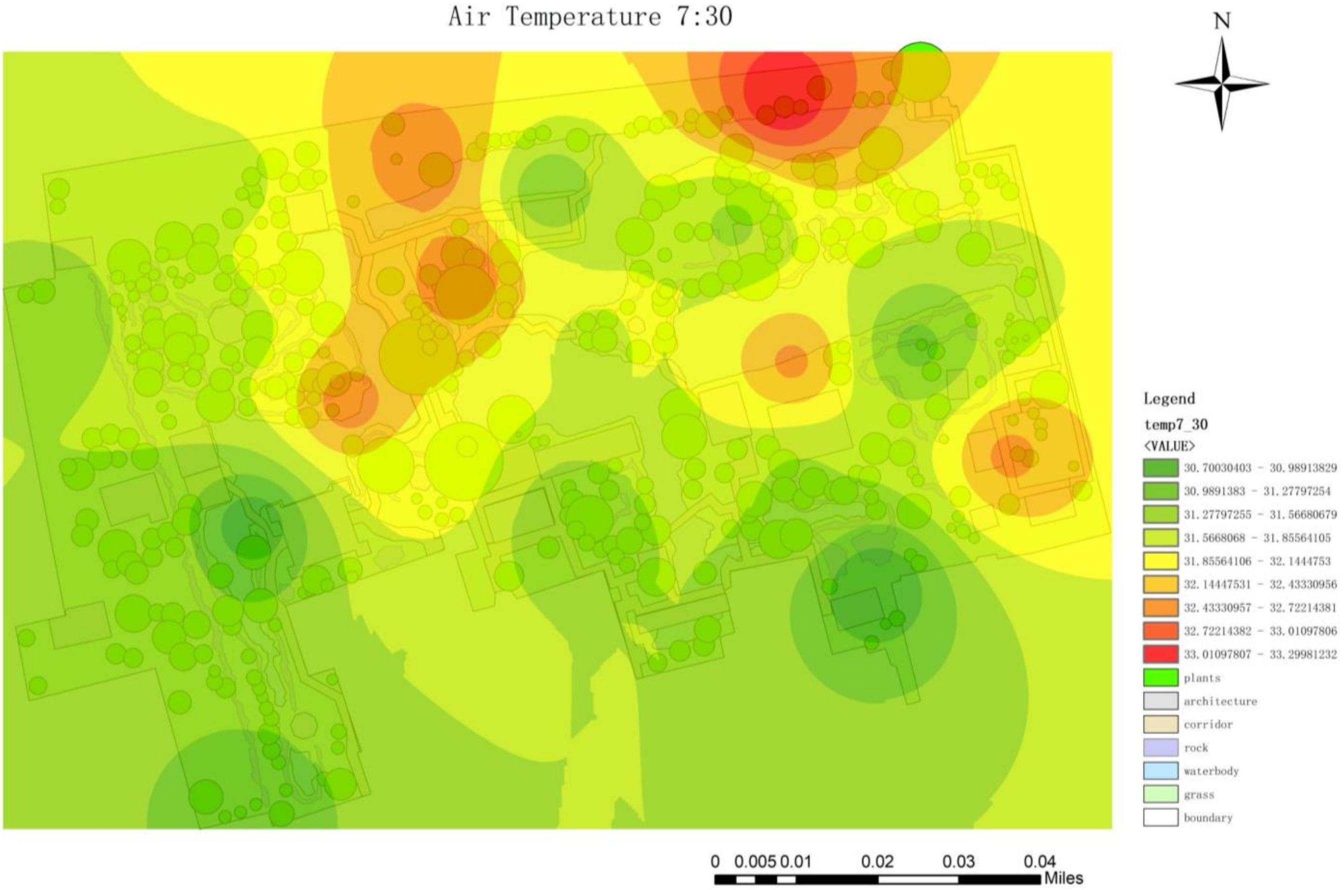

(a)

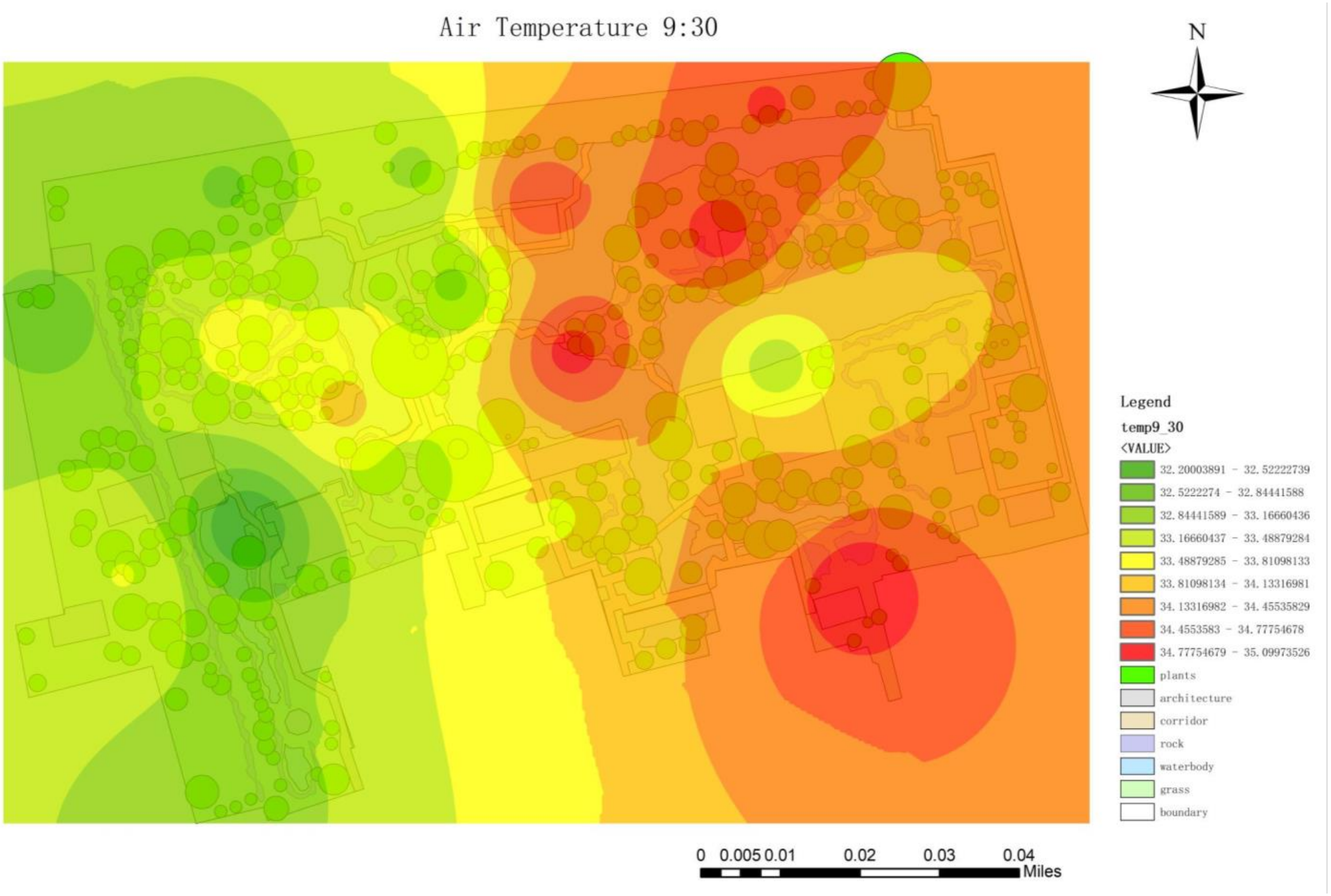
Air Temperature 9:30
N
Legend
temp9_30
<VALUE>
32. 20003891 - 32. 52222739
32. 5222274 - 32. 84441588
32. 84441589 - 33. 16660436
33. 16660437 - 33. 48879284
33. 48879285 - 33. 81098133
33. 81098134 - 34. 13316981
34. 13316982 - 34. 45535829
34. 4553583 - 34. 77754678
34. 77754679 - 35. 09973526
plants
architecture
corridor
rock
waterbody
grass
boundary
0 0.005 0.01 0.02 0.03 0.04
Miles

(b)

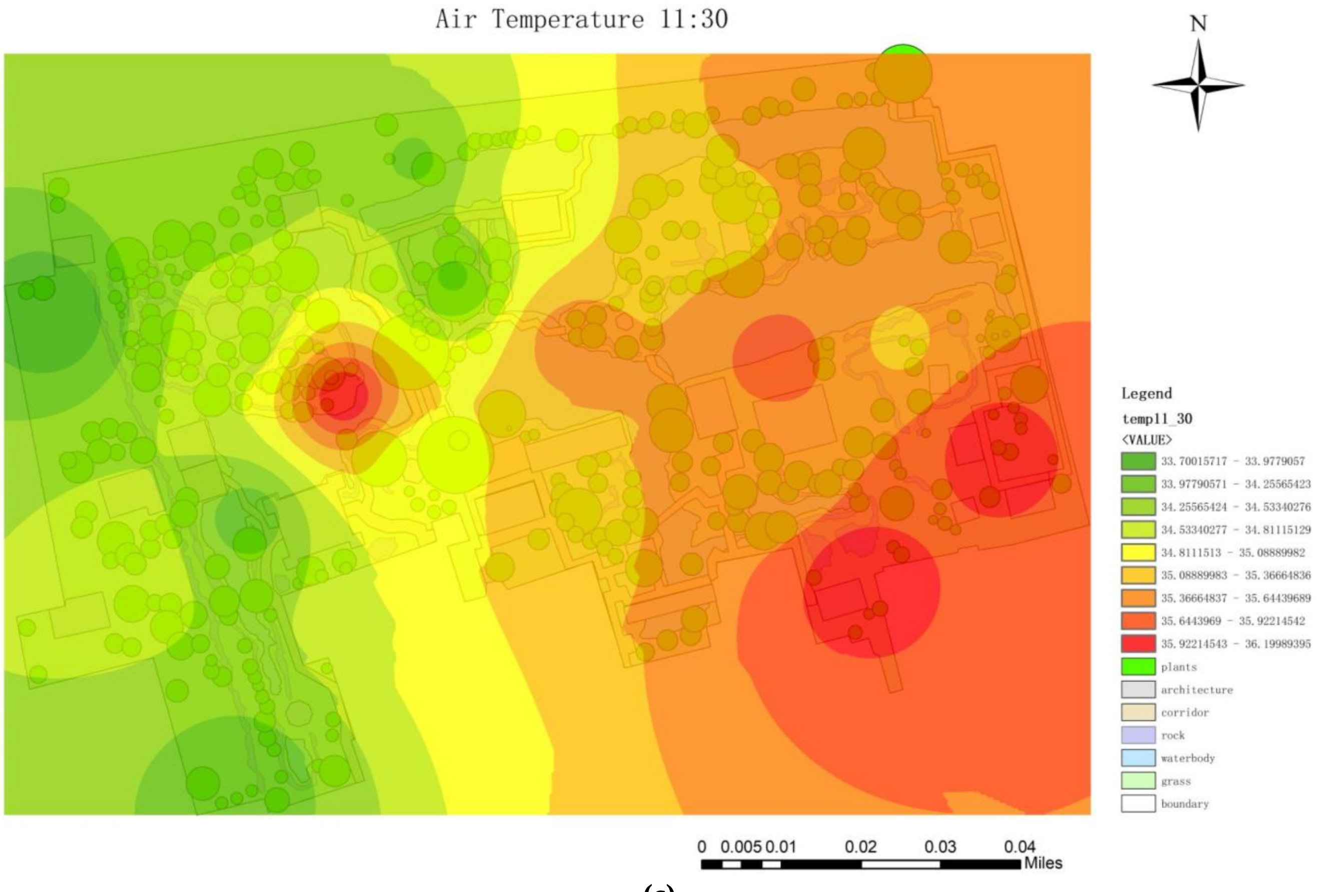
Air Temperature 11:30
N
Legend
temp11_30
<VALUE>
33. 70015717 - 33. 9779057
33. 97790571 - 34. 25565423
34. 25565424 - 34. 53340276
34. 53340277 - 34. 81115129
34. 8111513 - 35. 08889982
35. 08889983 - 35. 36664836
35. 36664837 - 35. 64439689
35. 6443969 - 35. 92214542
35. 92214543 - 36. 19989395
plants
architecture
corridor
rock
waterbody
grass
boundary
0 0.005 0.01 0.02 0.03 0.04
Miles

(c)

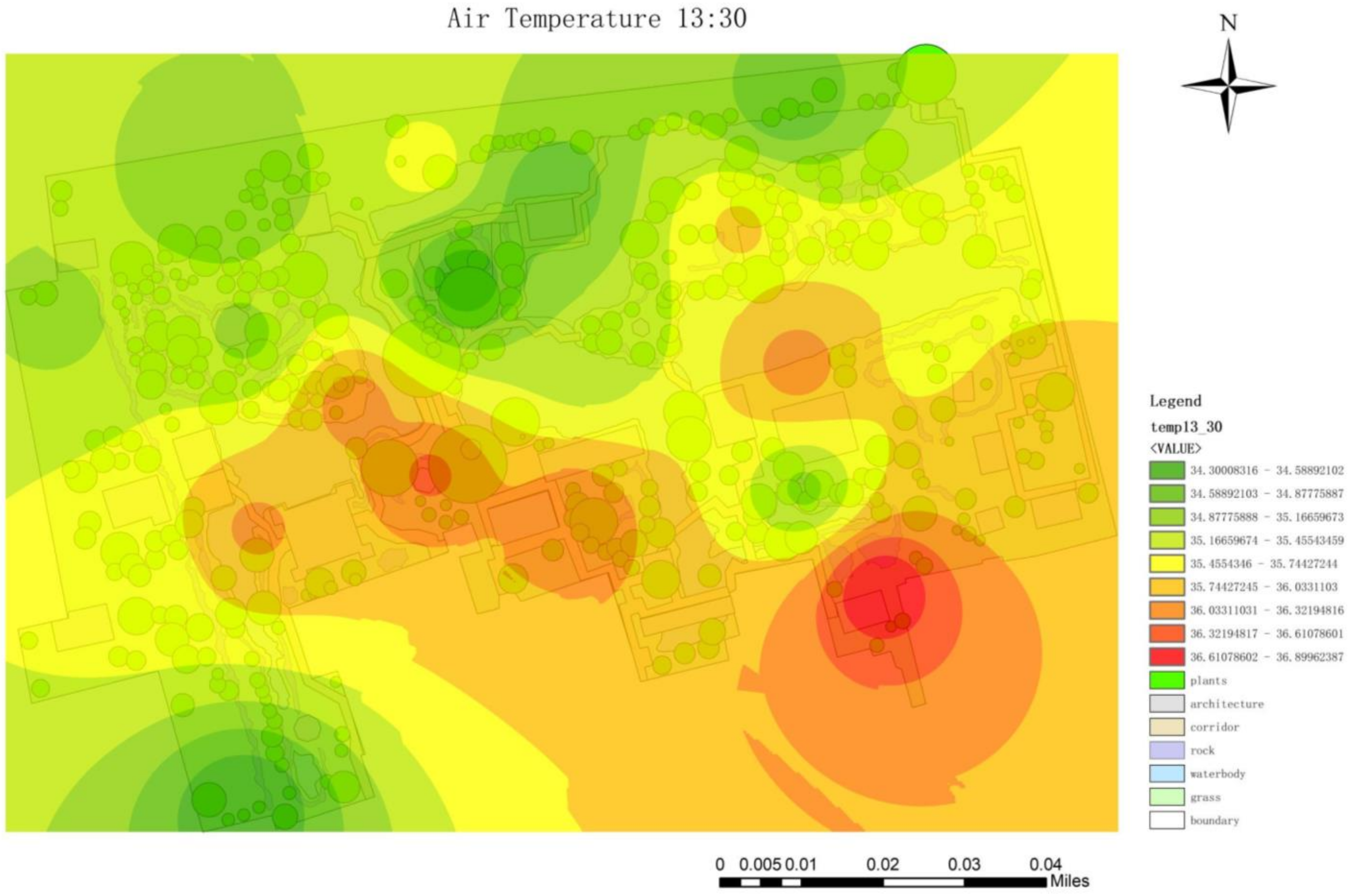
Air Temperature 13:30
N
Legend
temp13_30
<VALUE>
34.30008316 - 34.58892102
34.58892103 - 34.87775887
34.87775888 - 35.16659673
35.16659674 - 35.45543459
35.4554346 - 35.74427244
35.74427245 - 36.0331103
36.03311031 - 36.32194816
36.32194817 - 36.61078601
36.61078602 - 36.89962387
plants
architecture
corridor
rock
waterbody
grass
boundary
0 0.005 0.01 0.02 0.03 0.04
Miles

(d)

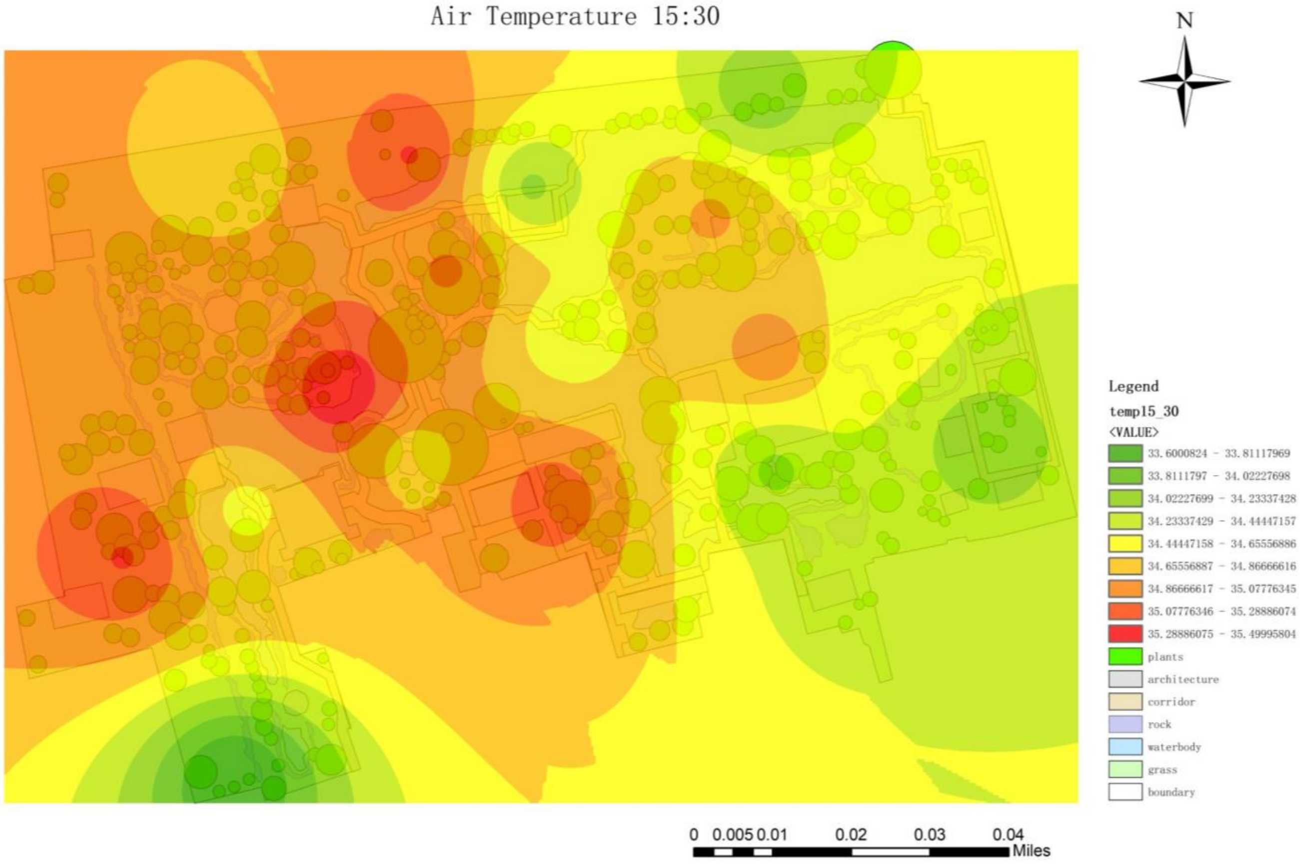
Air Temperature 15:30
N
Legend
temp15_30
<VALUE>
33.6000824 - 33.81117969
33.8111797 - 34.02227698
34.02227699 - 34.23337428
34.23337429 - 34.44447157
34.44447158 - 34.65556886
34.65556887 - 34.86666616
34.86666617 - 35.07776345
35.07776346 - 35.28886074
35.28886075 - 35.49995804
plants
architecture
corridor
rock
waterbody
grass
boundary
0 0.005 0.01 0.02 0.03 0.04
Miles

(e)

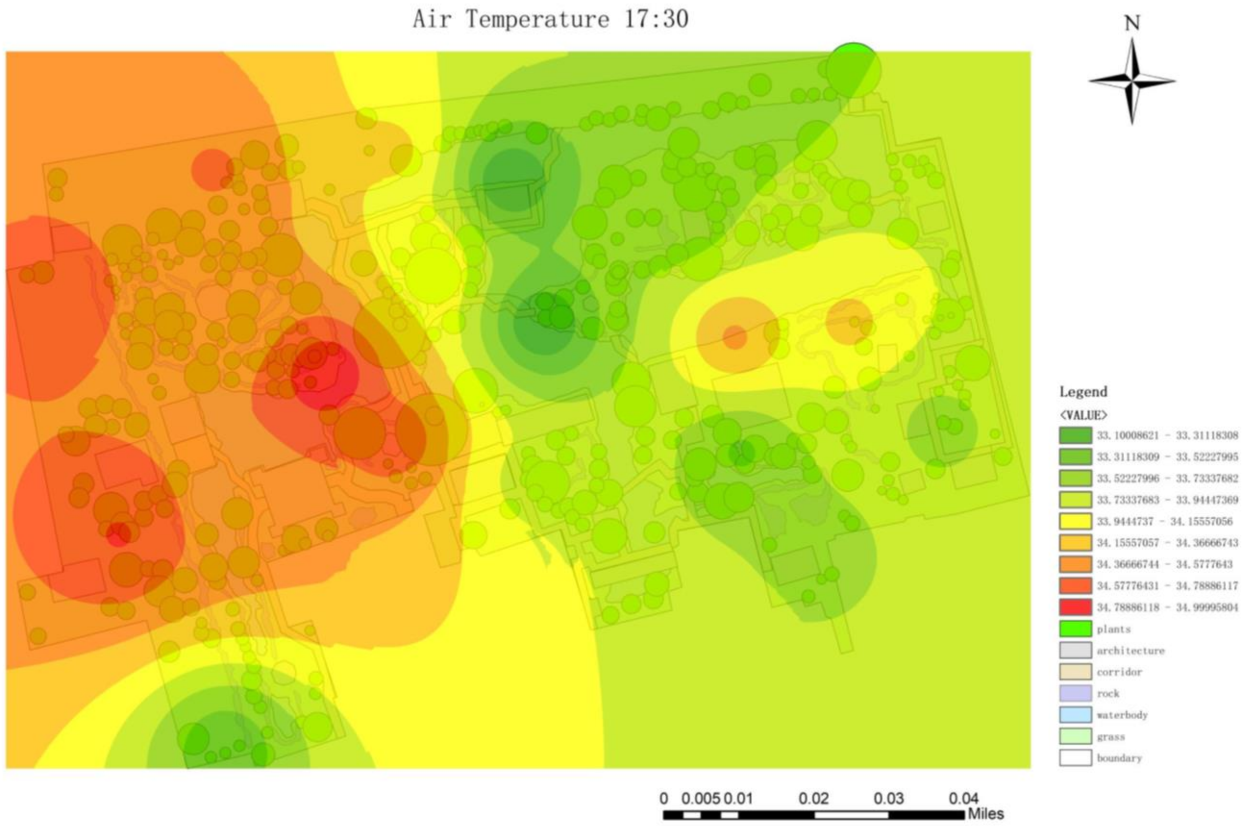

(f)

Figure 6. The scenario of air temperature from 7:30 to 17:30 in the Humble Administrator's Garden.

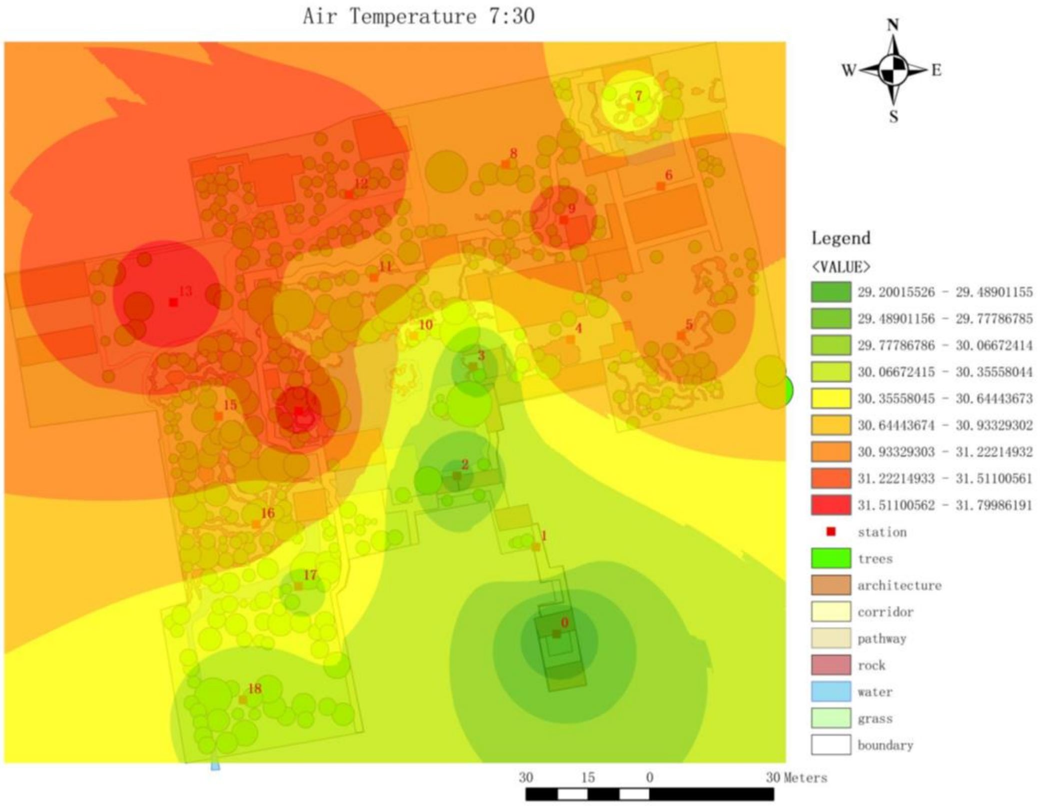

(a)

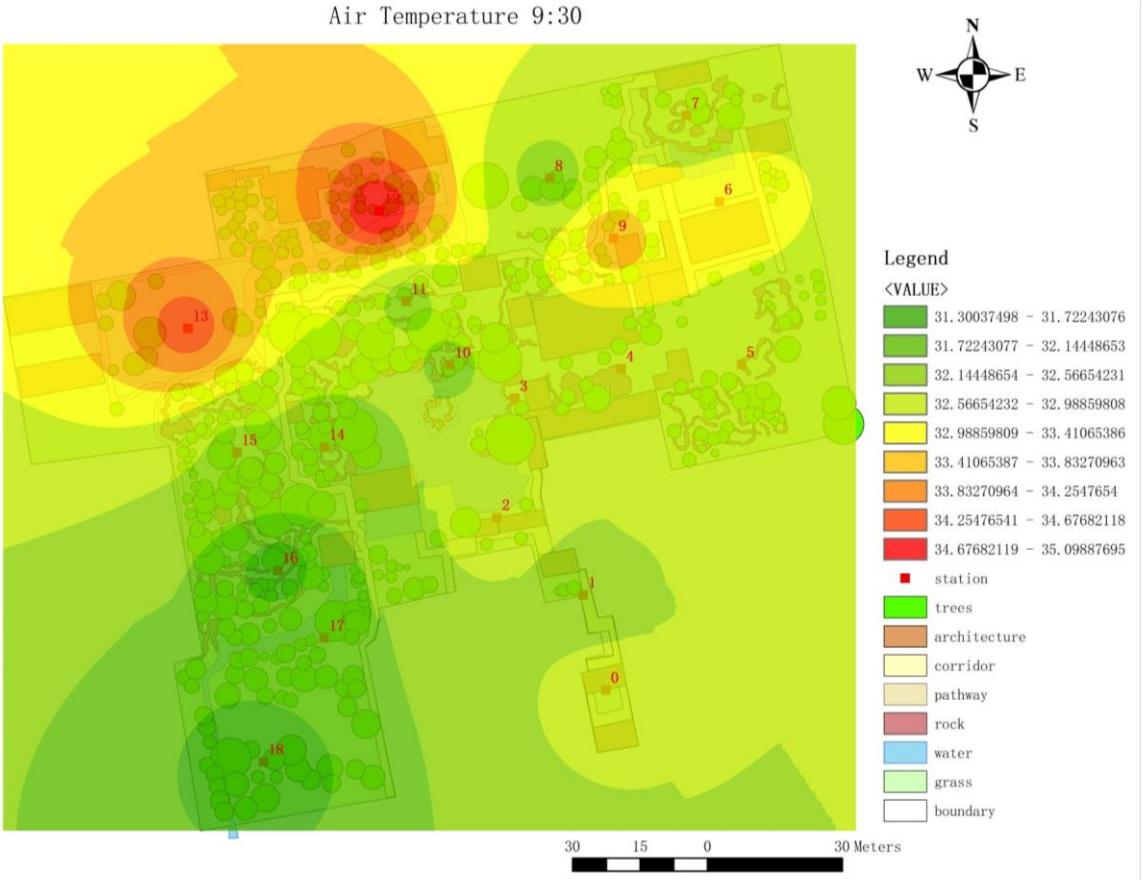
Air Temperature 9:30
N
W
E
S
Legend
<VALUE>
31.30037498 - 31.72243076
31.72243077 - 32.14448653
32.14448654 - 32.56654231
32.56654232 - 32.98859808
32.98859809 - 33.41065386
33.41065387 - 33.83270963
33.83270964 - 34.2547654
34.25476541 - 34.67682118
34.67682119 - 35.09887695
station
trees
architecture
corridor
pathway
rock
water
grass
boundary
30 15 0 30 Meters
0 1 2 3 4 5 6 7 8 9 10 11 12 13 14 15 16 17 18

(b)

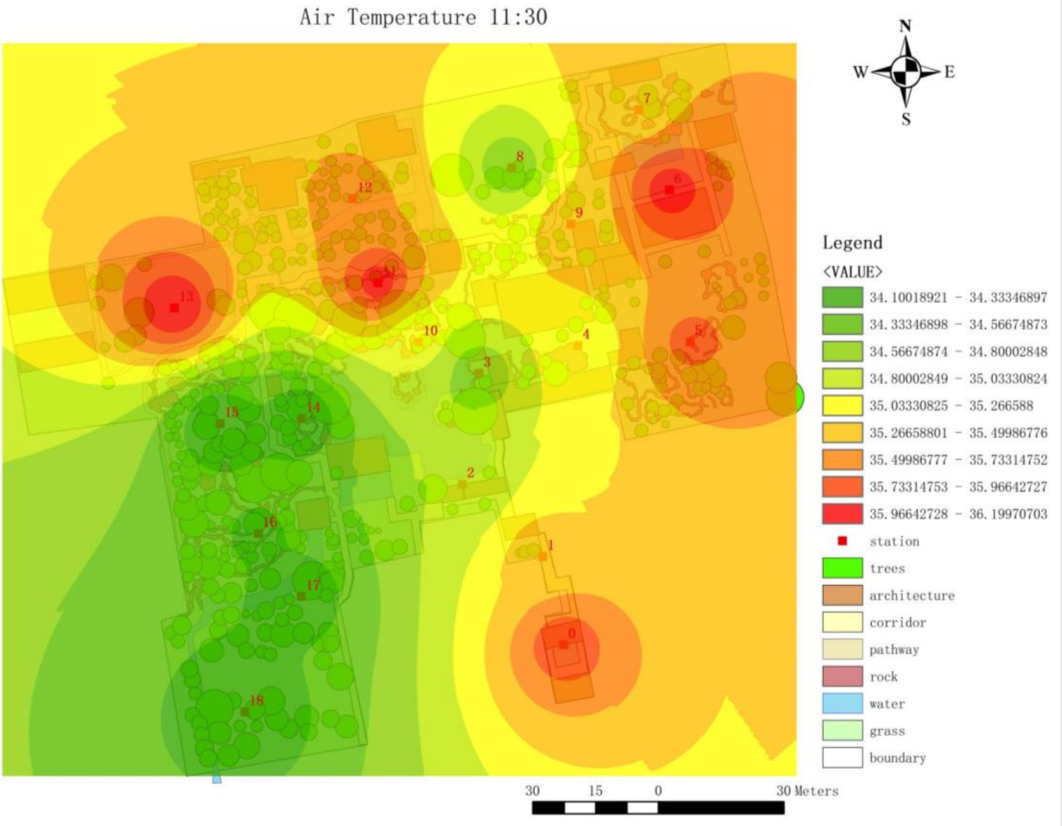
Air Temperature 11:30
N
W
E
S
Legend
<VALUE>
34.10018921 - 34.33346897
34.33346898 - 34.56674873
34.56674874 - 34.80002848
34.80002849 - 35.03330824
35.03330825 - 35.266588
35.26658801 - 35.49986776
35.49986777 - 35.73314752
35.73314753 - 35.96642727
35.96642728 - 36.19970703
station
trees
architecture
corridor
pathway
rock
water
grass
boundary
30 15 0 30 Meters
0 1 2 3 4 5 6 7 8 9 10 11 12 13 14 15 16 17 18

(c)

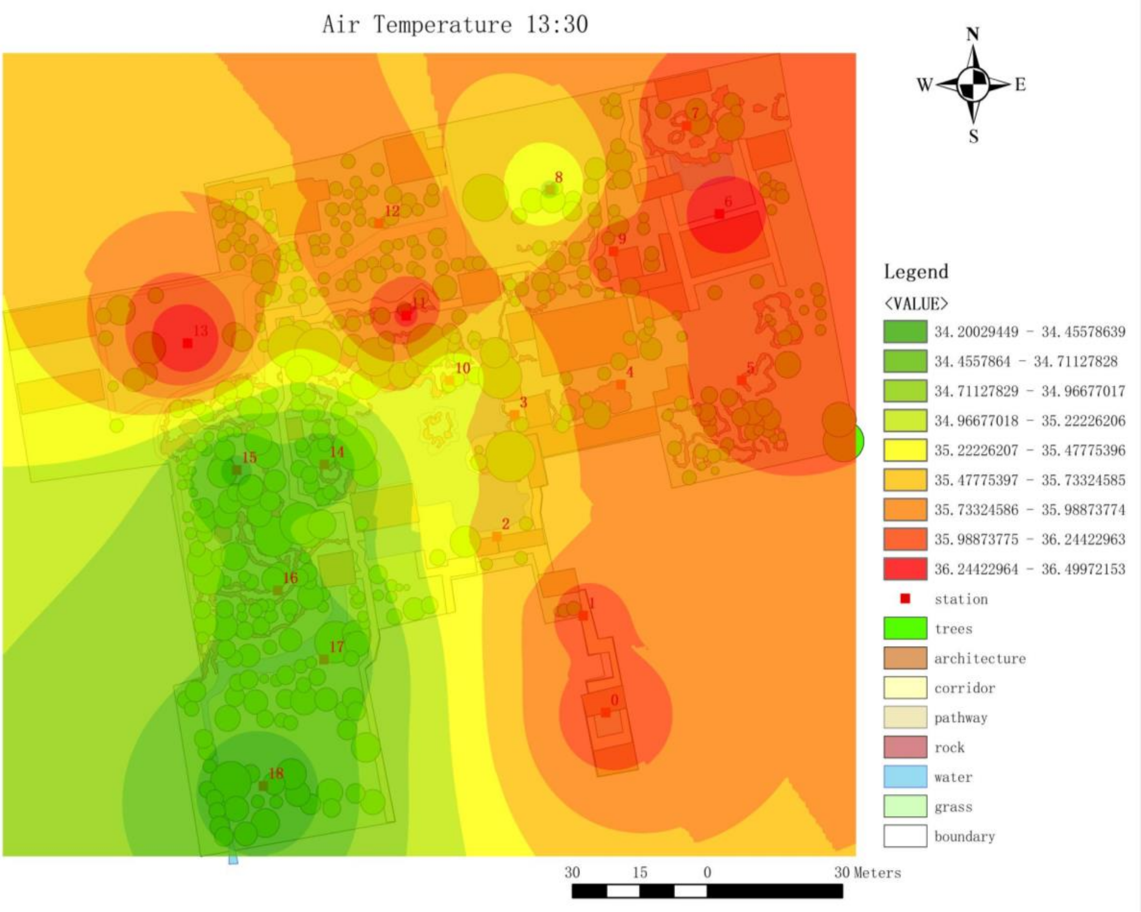
Air Temperature 13:30
N
W
E
S
Legend
<VALUE>
34.20029449 - 34.45578639
34.4557864 - 34.71127828
34.71127829 - 34.96677017
34.96677018 - 35.22226206
35.22226207 - 35.47775396
35.47775397 - 35.73324585
35.73324586 - 35.98873774
35.98873775 - 36.24422963
36.24422964 - 36.49972153
station
trees
architecture
corridor
pathway
rock
water
grass
boundary
0
1
2
3
4
5
6
7
8
9
10
11
12
13
14
15
16
17
18
30
15
0
30 Meters

(d)

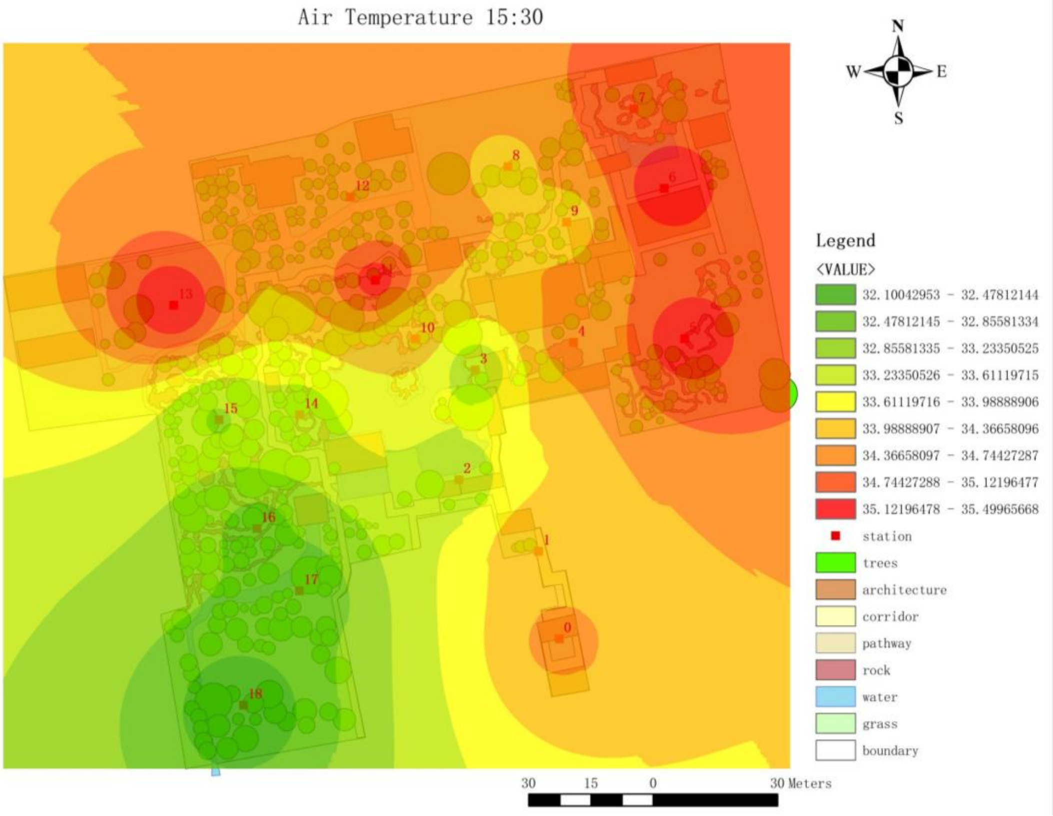
Air Temperature 15:30
N
W
E
S
Legend
<VALUE>
32.10042953 - 32.47812144
32.47812145 - 32.85581334
32.85581335 - 33.23350525
33.23350526 - 33.61119715
33.61119716 - 33.98888906
33.98888907 - 34.36658096
34.36658097 - 34.74427287
34.74427288 - 35.12196477
35.12196478 - 35.49965668
station
trees
architecture
corridor
pathway
rock
water
grass
boundary
0
1
2
3
4
6
7
8
9
10
12
13
14
15
16
17
18
30
15
0
30 Meters

(e)

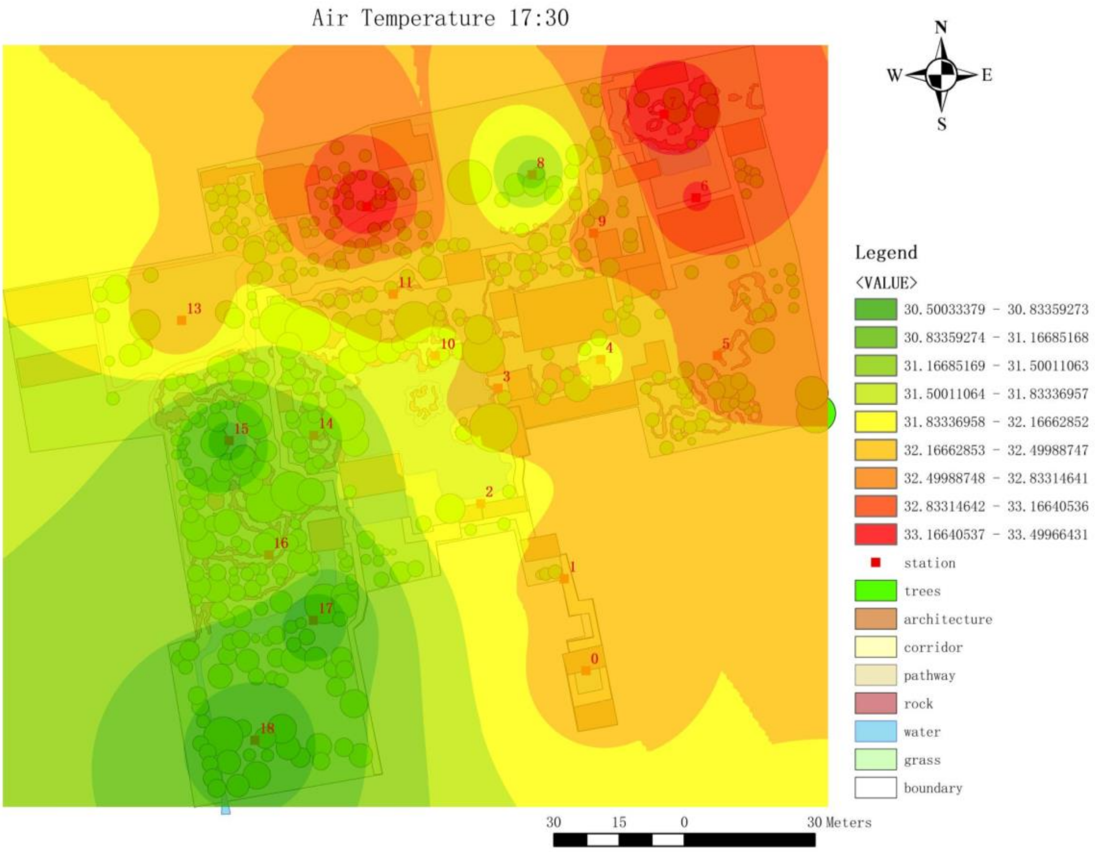

(f)

Figure 7. The scenario of air temperature from 7:30 to 17:30 in the Lingering Garden.

The Canglang Pavilion exhibited a similar pattern of temperature fluctuation, albeit on a smaller scale (**Figure 8**). In the early morning, air temperatures across the garden were relatively uniform, around 32 ℃, with cooler readings at stations 7, 8, and 9, located near vegetation and water bodies. As the day progressed, temperatures increased, especially at stations exposed to direct sunlight or architectural elements, such as station 1, which reached approximately 33.6 ℃. By midday, air temperatures across the garden rose sharply, with stations in sunlit areas, like station 4, recording the highest values (34–35.5 ℃). Water-adjacent stations, such as 3, continued to benefit from evaporative cooling, while stations with dense vegetation, like 7, remained comparatively cool even during peak heat. As temperatures began to decline in the evening, stations near water features and dense vegetation cooled more rapidly, whereas exposed pathways and hardscapes, such as station 4, retained heat for longer durations.

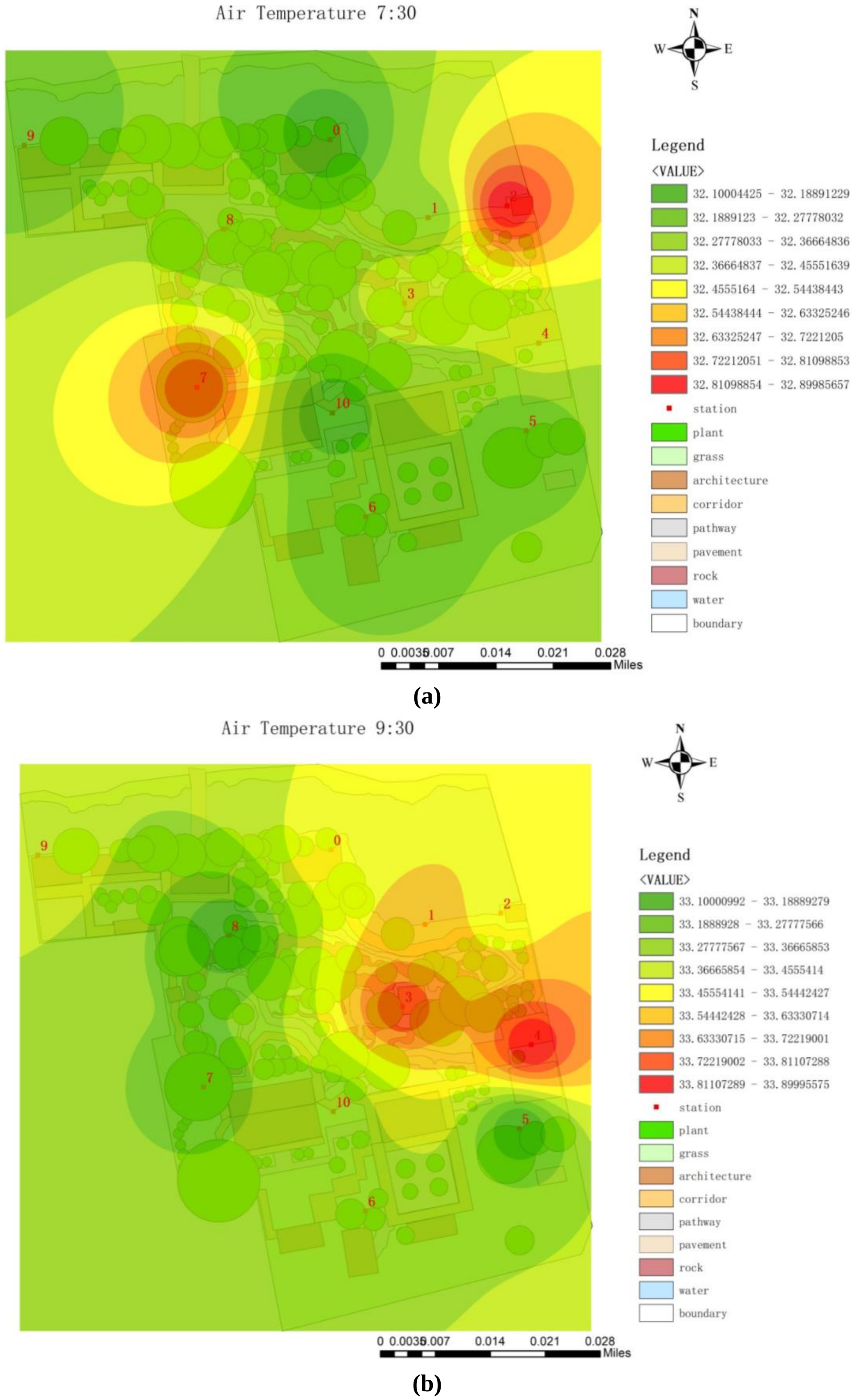
Air Temperature 7:30
N
W
E
S
Legend
<VALUE>
32.10004425 - 32.18891229
32.1889123 - 32.27778032
32.27778033 - 32.36664836
32.36664837 - 32.45551639
32.4555164 - 32.54438443
32.54438444 - 32.63325246
32.63325247 - 32.7221205
32.72212051 - 32.81098853
32.81098854 - 32.89985657
station
plant
grass
architecture
corridor
pathway
pavement
rock
water
boundary
0 0.0035 0.007 0.014 0.021 0.028
Miles
0
1
2
3
4
5
6
7
8
9
10
Air Temperature 9:30
Legend
<VALUE>
33.10000992 - 33.18889279
33.1888928 - 33.27777566
33.27777567 - 33.36665853
33.36665854 - 33.4555414
33.45554141 - 33.54442427
33.54442428 - 33.63330714
33.63330715 - 33.72219001
33.72219002 - 33.81107288
33.81107289 - 33.89995575
station
plant
grass
architecture
corridor
pathway
pavement
rock
water
boundary

(a)

(b)

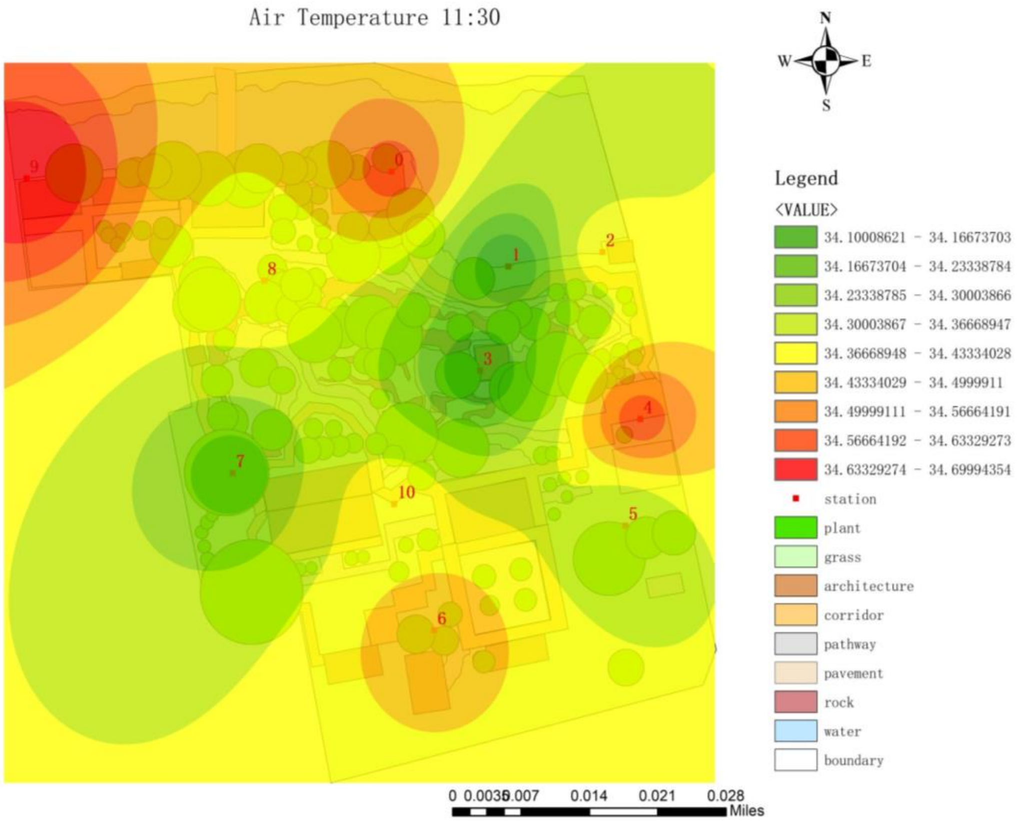
Air Temperature 11:30
N
W
E
S
9
0
1
2
8
3
4
7
10
5
6
Legend
<VALUE>
34. 10008621 – 34. 16673703
34. 16673704 – 34. 23338784
34. 23338785 – 34. 30003866
34. 30003867 – 34. 36668947
34. 36668948 – 34. 43334028
34. 43334029 – 34. 4999911
34. 49999111 – 34. 56664191
34. 56664192 – 34. 63329273
34. 63329274 – 34. 69994354
station
plant
grass
architecture
corridor
pathway
pavement
rock
water
boundary
0 0.0035 0.007 0.014 0.021 0.028
Miles

(c)

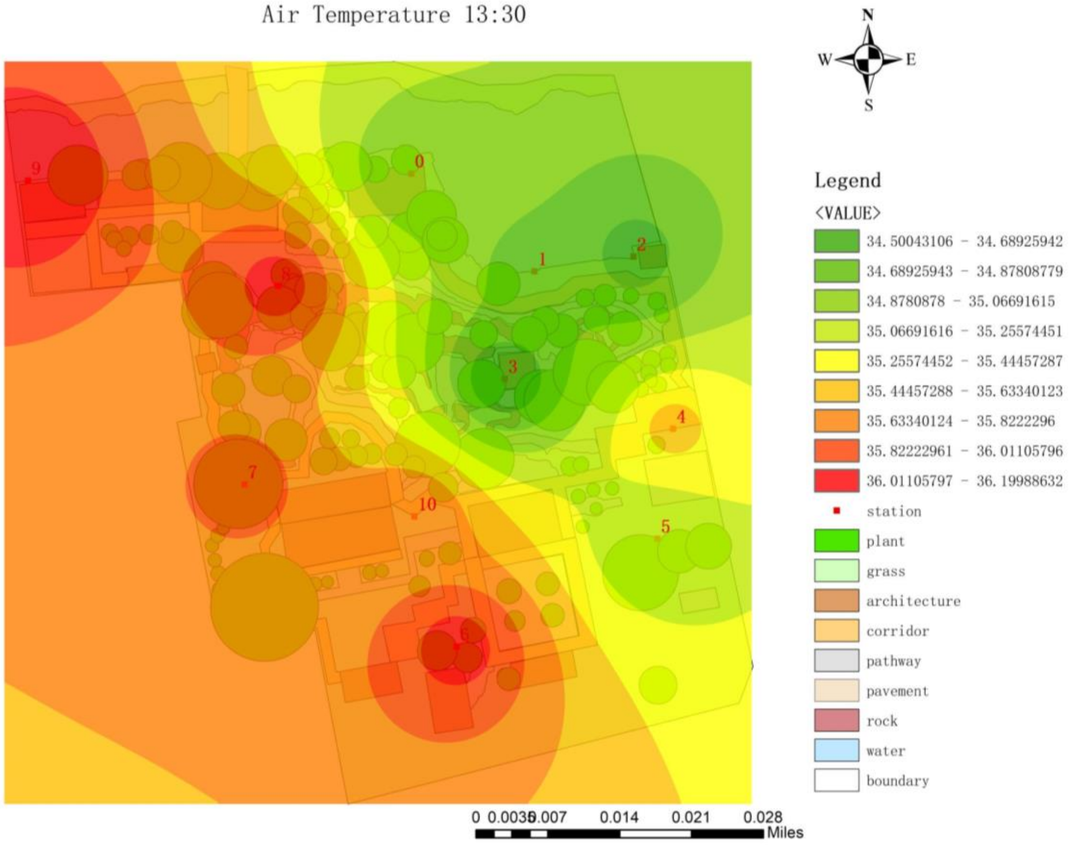
Air Temperature 13:30
N
W
E
S
9
0
1
2
8
3
4
7
10
5
6
Legend
<VALUE>
34. 50043106 – 34. 68925942
34. 68925943 – 34. 87808779
34. 8780878 – 35. 06691615
35. 06691616 – 35. 25574451
35. 25574452 – 35. 44457287
35. 44457288 – 35. 63340123
35. 63340124 – 35. 8222296
35. 82222961 – 36. 01105796
36. 01105797 – 36. 19988632
station
plant
grass
architecture
corridor
pathway
pavement
rock
water
boundary
0 0.0035 0.007 0.014 0.021 0.028
Miles

(d)

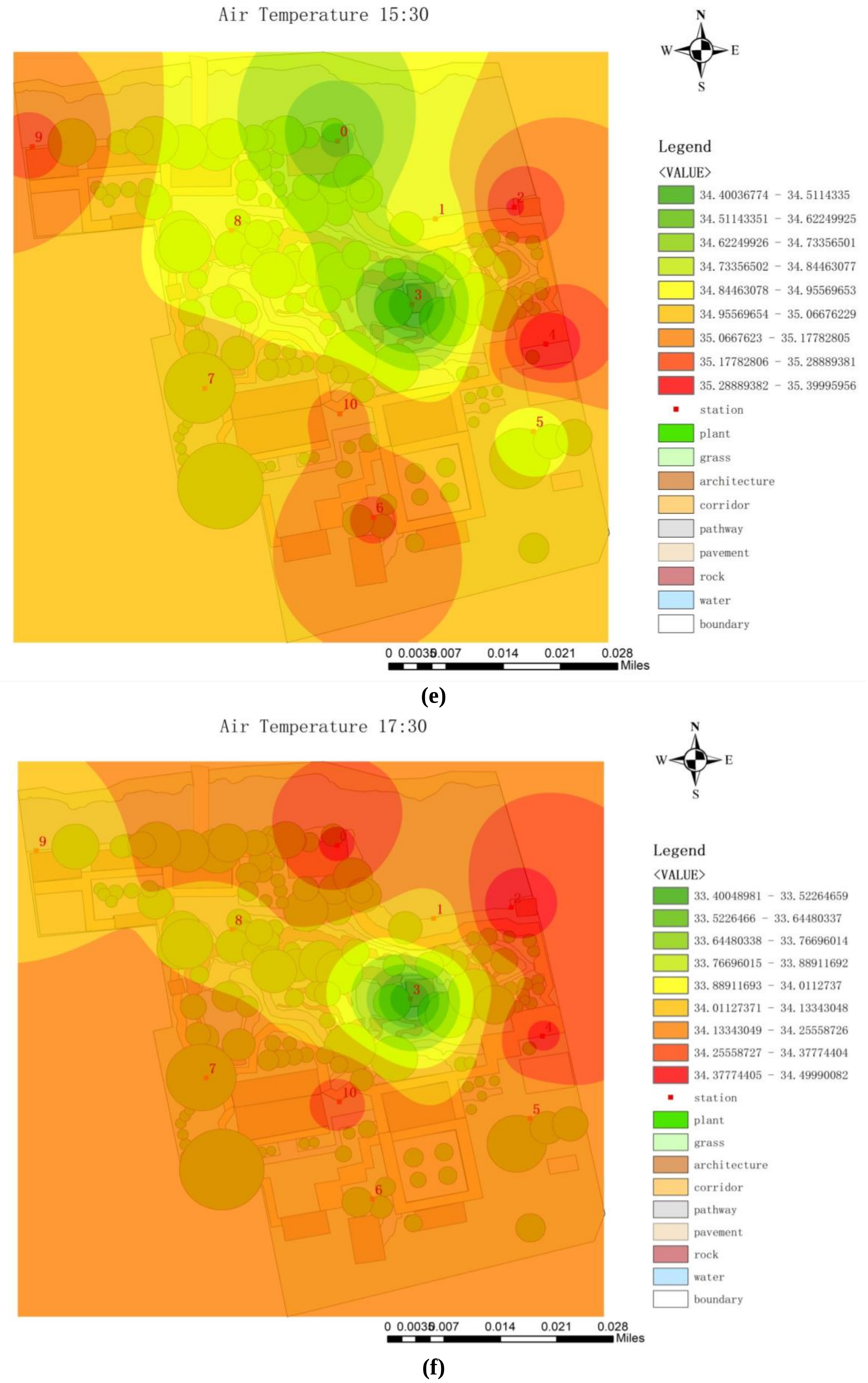

Figure 8. The scenario of air temperature from 7:30 to 17:30 in the Canglang Pavilion.

It can be seen that in all three gardens, the water bodies and dense vegetation consistently provide a cooling effect, significantly lowering temperatures. The size and layout of the water features, as well as the density and type of vegetation, play a crucial role in the magnitude of this cooling effect. In addition, the presence of rockeries and architectural structures tends to retain heat, creating unique thermal zones within the garden. These findings suggest that the design of traditional Chinese gardens employs a common microclimate regulation strategy. Factor weighting analyses showed that in the Humble Administrator's Garden, the Lingering Garden, and the Canglang Pavilion, water bodies had the most significant effect on reducing temperature, with a much higher weight than vegetation and architectural structures. Especially in the high temperature period, the cooling effect of water bodies is especially obvious, which can significantly reduce the air temperature in the surrounding area.

4.2. Impact of landscape elements on relative humidity

Relative humidity levels followed an inverse pattern to temperature fluctuations, generally decreasing from morning to midday before gradually rising again in the late afternoon (**Figure 9**). In the Humble Administrator's Garden, humidity levels were highest in the morning, particularly near water bodies and dense vegetation, with elevated readings at stations 12 and 16. As the day progressed, humidity declined significantly in sun-exposed areas lacking vegetation, such as stations 3 and 9. In contrast, zones with water features and dense foliage retained higher humidity, though at lower levels than morning readings. Late afternoon and evening measurements indicated a rebound in humidity levels, especially near water features (e.g., stations 12 and 14), where water evaporation contributed to increased ambient moisture.

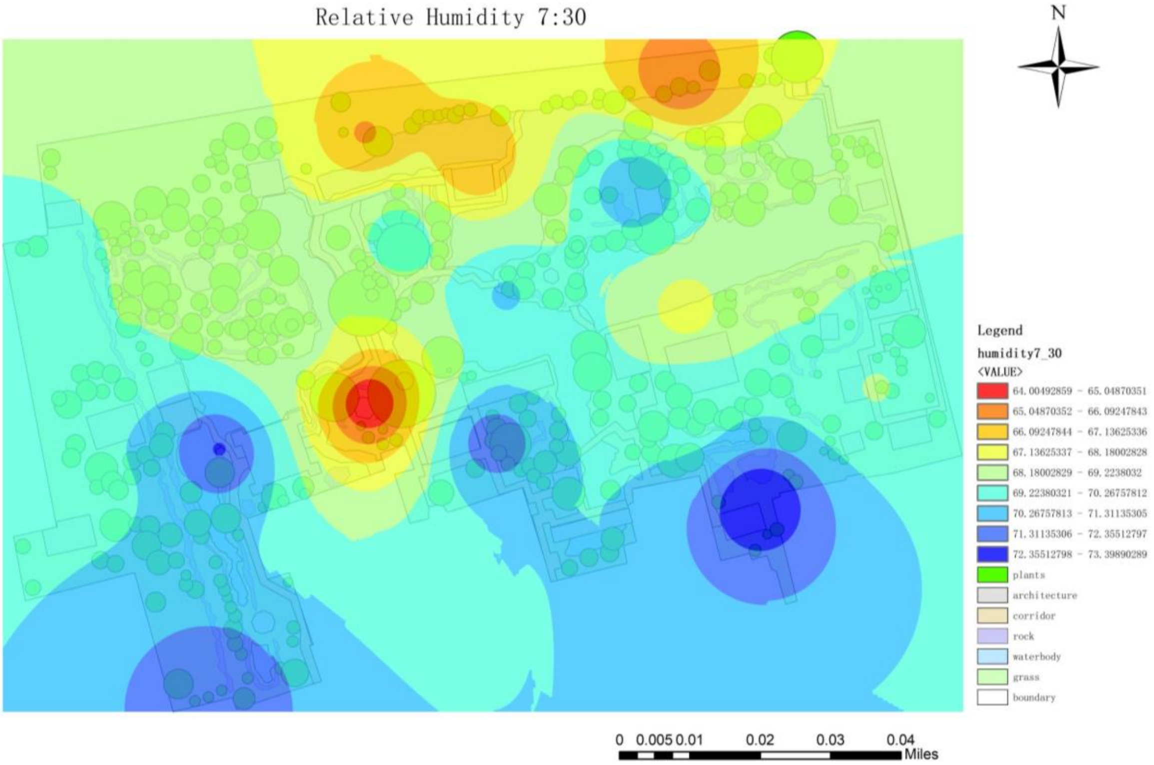

(a)

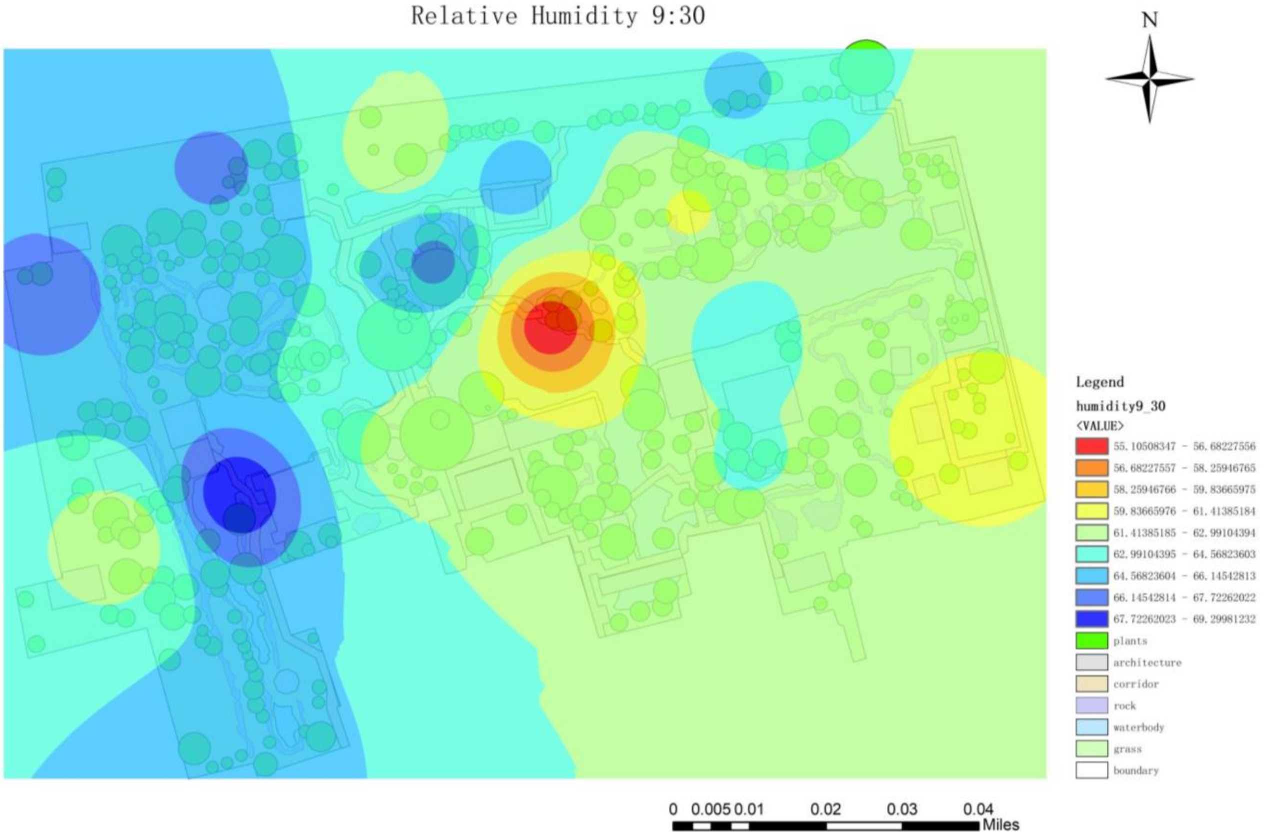
Relative Humidity 9:30
N
Legend
humidity9_30
<VALUE>
🟥 55.10508347 - 56.68227556
🟧 56.68227557 - 58.25946765
🟨 58.25946766 - 59.83665975
🟨 59.83665976 - 61.41385184
🟩 61.41385185 - 62.99104394
🟦 62.99104395 - 64.56823603
🟦 64.56823604 - 66.14542813
🟦 66.14542814 - 67.72262022
🟦 67.72262023 - 69.29981232
🟩 plants
⬜ architecture
🟫 corridor
🟪 rock
🟦 waterbody
🟩 grass
⬜ boundary
0 0.005 0.01 0.02 0.03 0.04
Miles

(b)

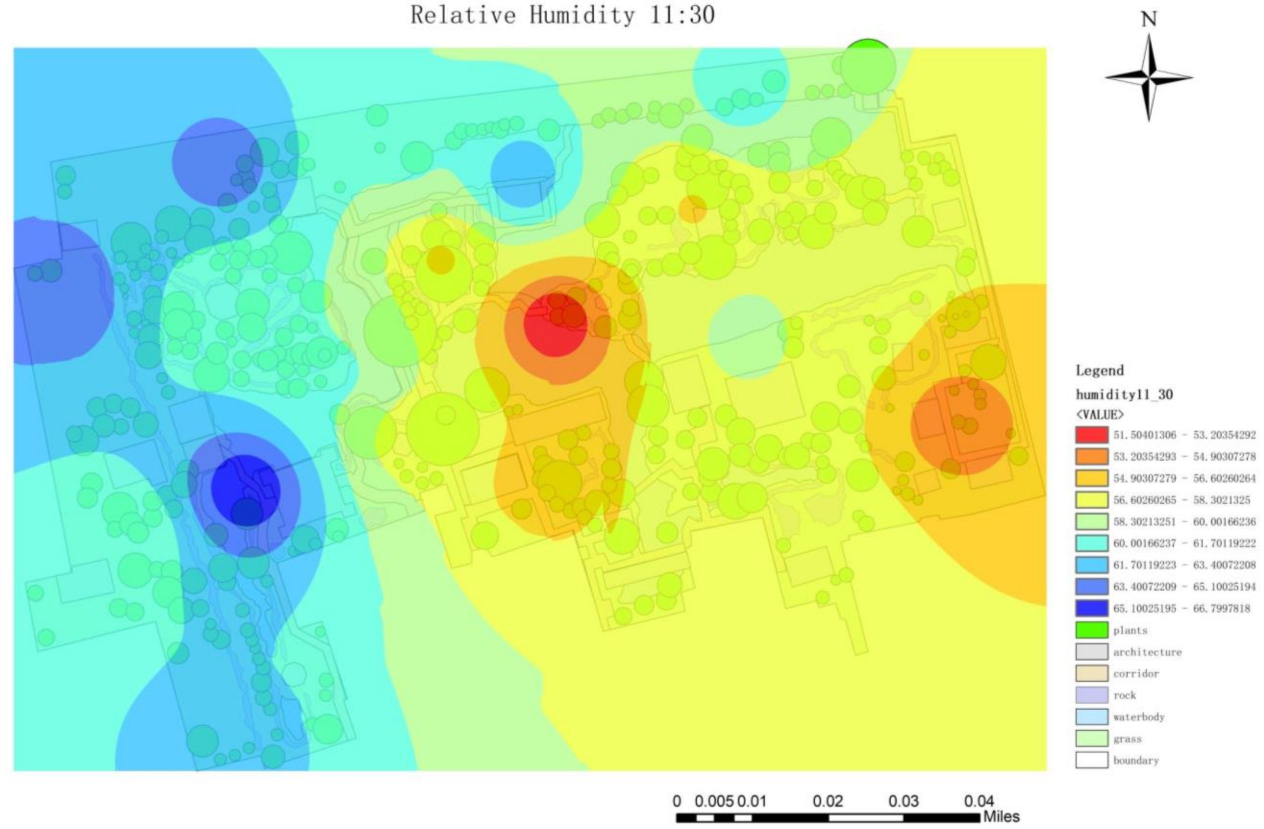
Relative Humidity 11:30
N
Legend
humidity11_30
<VALUE>
🟥 51.50401306 - 53.20354292
🟧 53.20354293 - 54.90307278
🟨 54.90307279 - 56.60260264
🟨 56.60260265 - 58.3021325
🟩 58.30213251 - 60.00166236
🟦 60.00166237 - 61.70119222
🟦 61.70119223 - 63.40072208
🟦 63.40072209 - 65.10025194
🟦 65.10025195 - 66.7997818
🟩 plants
⬜ architecture
🟫 corridor
🟪 rock
🟦 waterbody
🟩 grass
⬜ boundary
0 0.005 0.01 0.02 0.03 0.04
Miles

(c)

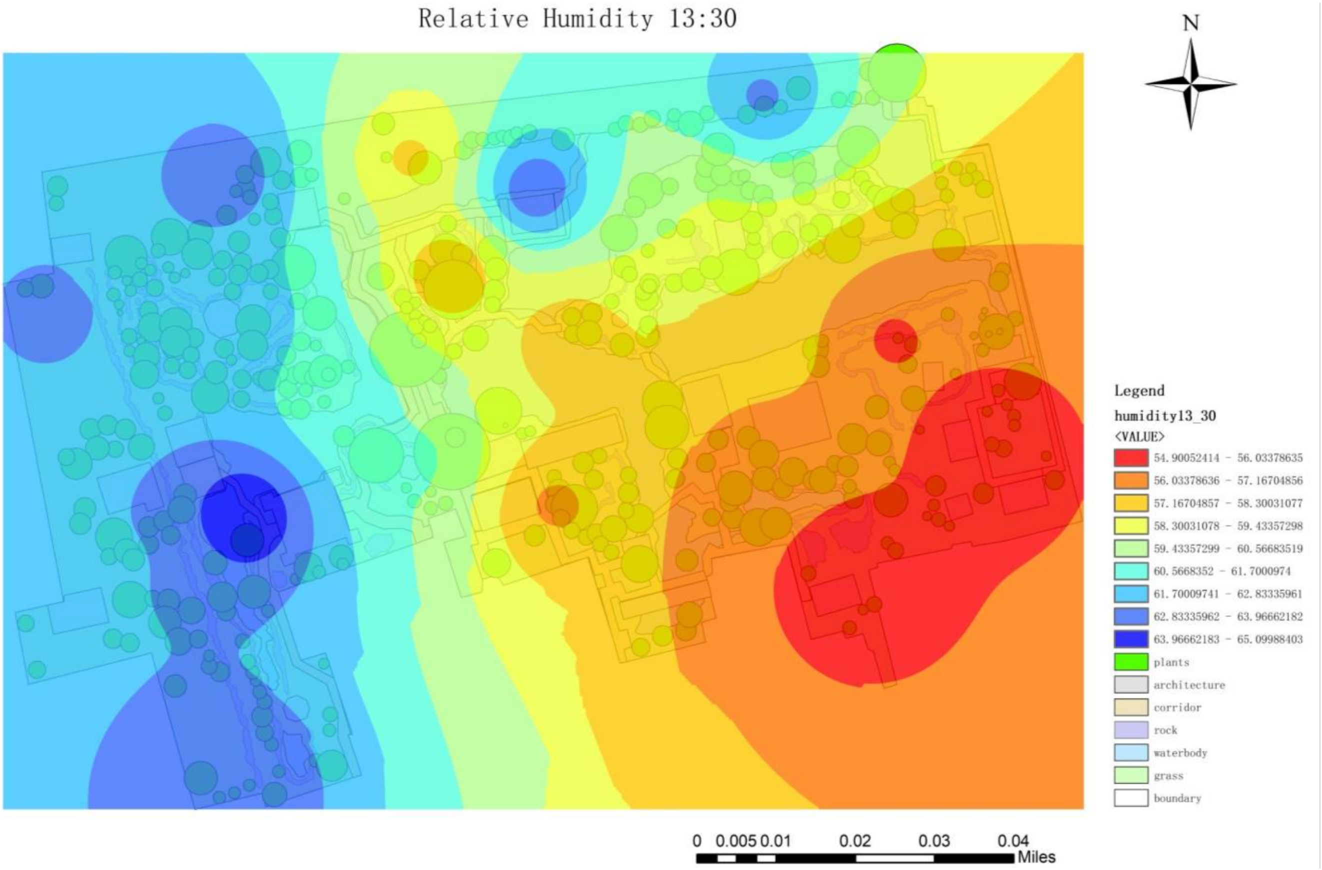
Relative Humidity 13:30
N
Legend
humidity13_30
<VALUE>
🟥 54.90052414 - 56.03378635
🟧 56.03378636 - 57.16704856
🟨 57.16704857 - 58.30031077
🟨 58.30031078 - 59.43357298
🟩 59.43357299 - 60.56683519
🟦 60.5668352 - 61.7000974
🟦 61.70009741 - 62.83335961
🟦 62.83335962 - 63.96662182
🟦 63.96662183 - 65.09988403
🟩 plants
⬜ architecture
⬜ corridor
⬜ rock
⬜ waterbody
🟩 grass
⬜ boundary
0 0.005 0.01 0.02 0.03 0.04
Miles

(d)

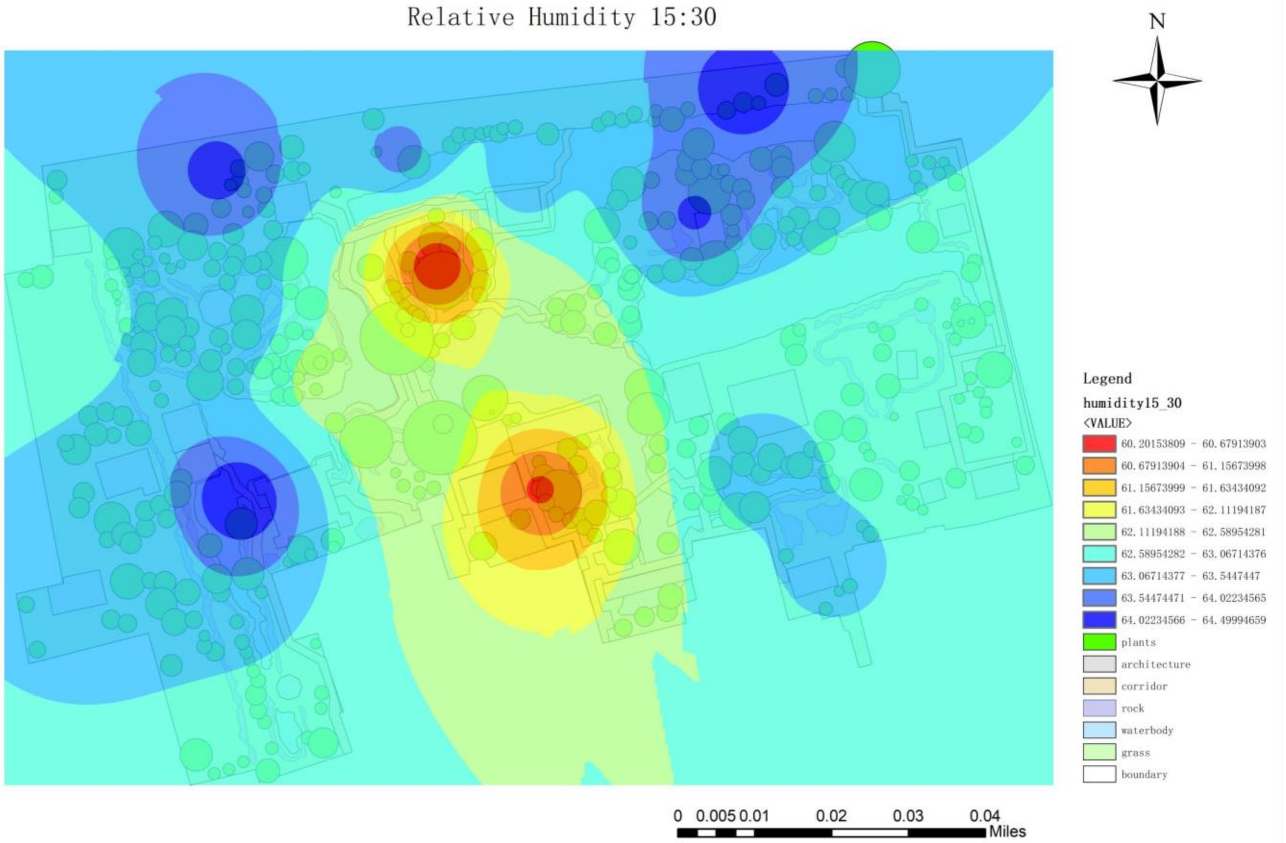
Relative Humidity 15:30
N
Legend
humidity15_30
<VALUE>
🟥 60.20153809 - 60.67913903
🟧 60.67913904 - 61.15673998
🟨 61.15673999 - 61.63434092
🟨 61.63434093 - 62.11194187
🟩 62.11194188 - 62.58954281
🟦 62.58954282 - 63.06714376
🟦 63.06714377 - 63.5447447
🟦 63.54474471 - 64.02234565
🟦 64.02234566 - 64.49994659
🟩 plants
⬜ architecture
⬜ corridor
⬜ rock
⬜ waterbody
🟩 grass
⬜ boundary
0 0.005 0.01 0.02 0.03 0.04
Miles

(e)

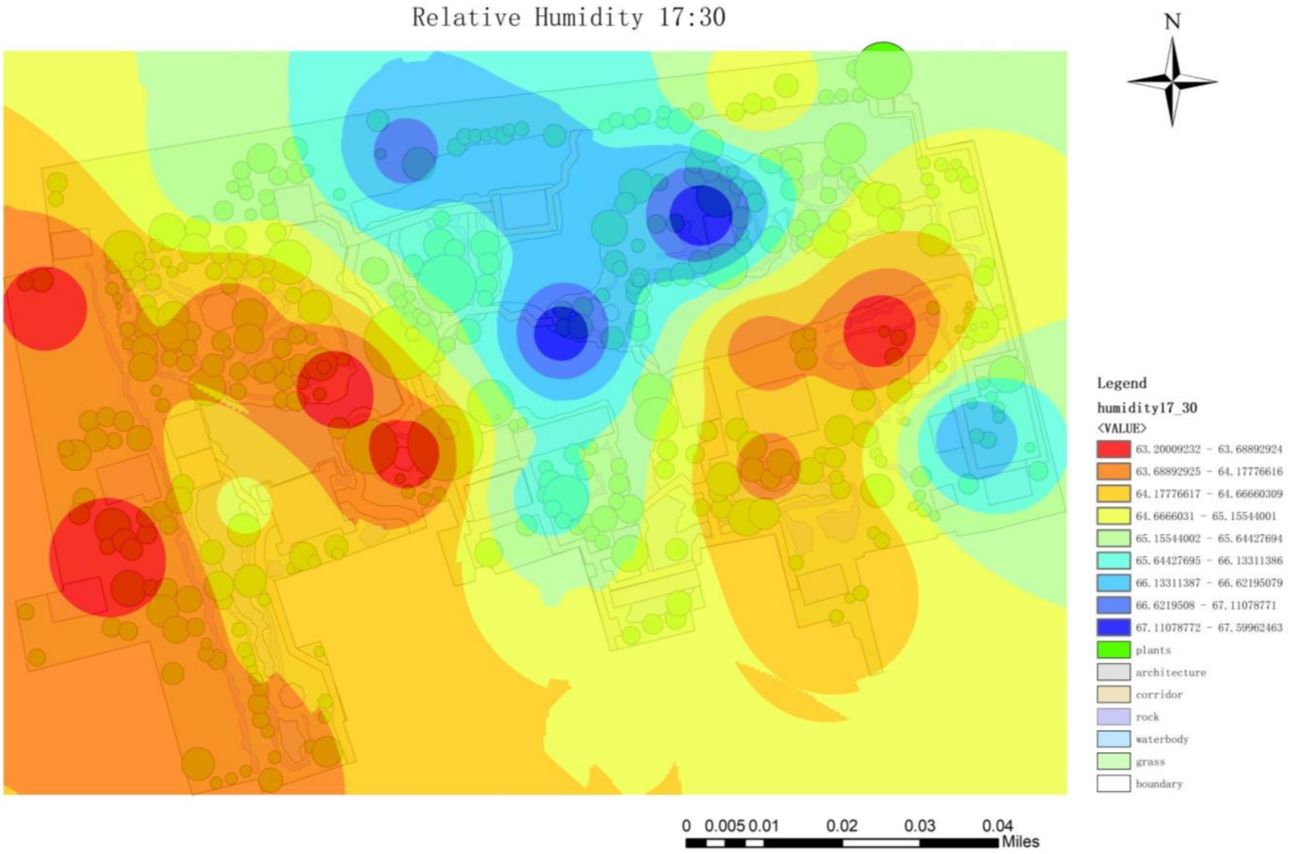

(f)

Figure 9. Relative humidity scenarios from 7:30 to 17:30 in the Humble Administrator’s Garden.

In the morning of Lingering Garden, station 18 consistently shows high humidity levels in the early morning (**Figure 10**). The proximity to dense vegetation and water features likely contributes to this. Vegetation retains moisture overnight, and the cooling effect of water bodies keeps humidity high during the morning hours. Station 17 and 16 show higher humidity due to dense foliage and water features that maintain high humidity levels by reducing air circulation and trapping moisture. Station 11 area near the central pond shows moderate humidity. The presence of open water helps to increase local humidity, but the presence of architectural structures and pathways allows for more air movement, preventing the buildup of humidity to the levels seen in more enclosed vegetated areas. Station 0, 1, 2 areas show relatively lower humidity in the morning, which can be attributed to exposure to sunlight and reduced vegetation cover. These areas are more open, allowing for greater air circulation, which reduces relative humidity.

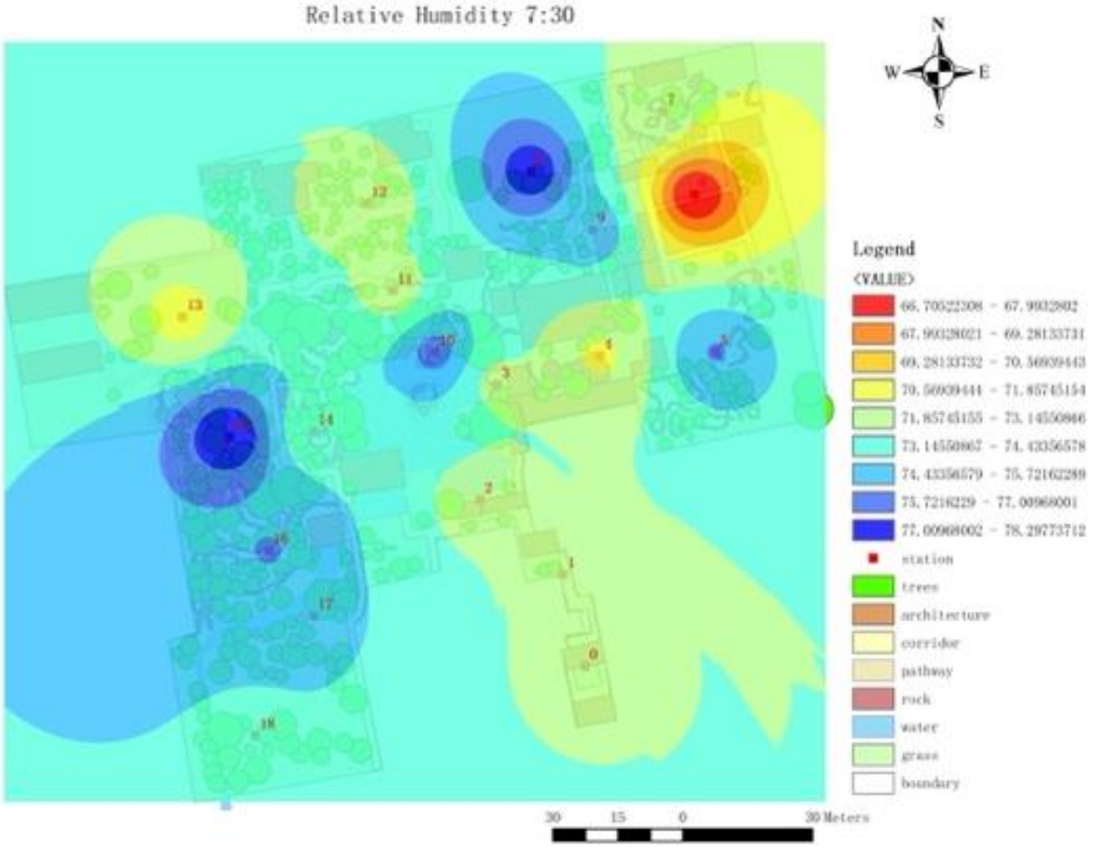
Relative Humidity 7:30
N
W
E
S
Legend
<VALUE>
🟥 66.70522308 - 67.9932802
🟧 67.99328021 - 69.28133731
🟧 69.28133732 - 70.56939443
🟨 70.56939444 - 71.85745154
🟩 71.85745155 - 73.14550866
🟦 73.14550867 - 74.43356578
🟦 74.43356579 - 75.72162289
🟦 75.7216229 - 77.00968001
🟦 77.00968002 - 78.29773712
■ station
🟩 trees
🟫 architecture
🟨 corridor
🟨 pathway
🟥 rock
🟦 water
🟩 grass
☐ boundary
30 15 0 30 Meters
0
1
2
3
4
5
7
9
10
11
12
13
14
16
17
18

(a)

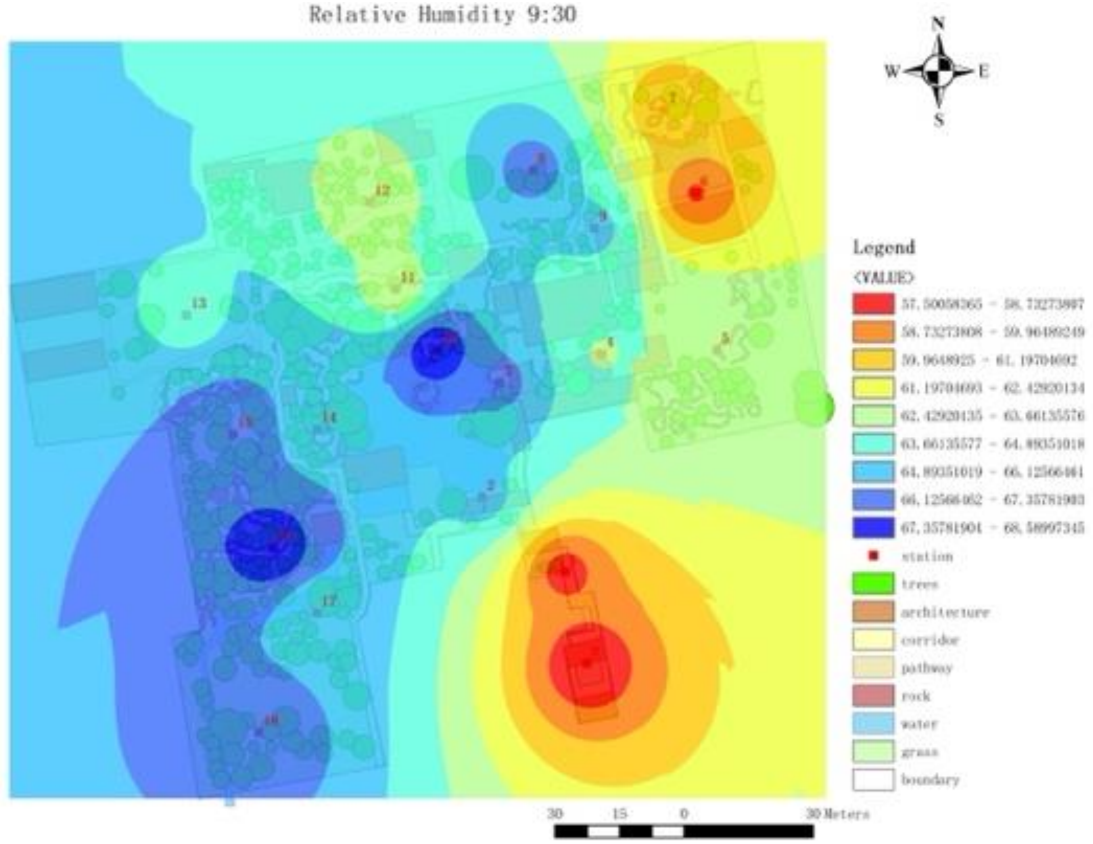
Relative Humidity 9:30
N
W
E
S
Legend
<VALUE>
🟥 57.50058365 - 58.73273807
🟧 58.73273808 - 59.96489249
🟧 59.9648925 - 61.19704692
🟨 61.19704693 - 62.42920134
🟩 62.42920135 - 63.66135576
🟦 63.66135577 - 64.89351018
🟦 64.89351019 - 66.12566461
🟦 66.12566462 - 67.35781903
🟦 67.35781904 - 68.58997345
■ station
🟩 trees
🟫 architecture
🟨 corridor
🟨 pathway
🟥 rock
🟦 water
🟩 grass
☐ boundary
30 15 0 30 Meters
2
4
5
7
9
11
12
13
14
15
16
17

(b)

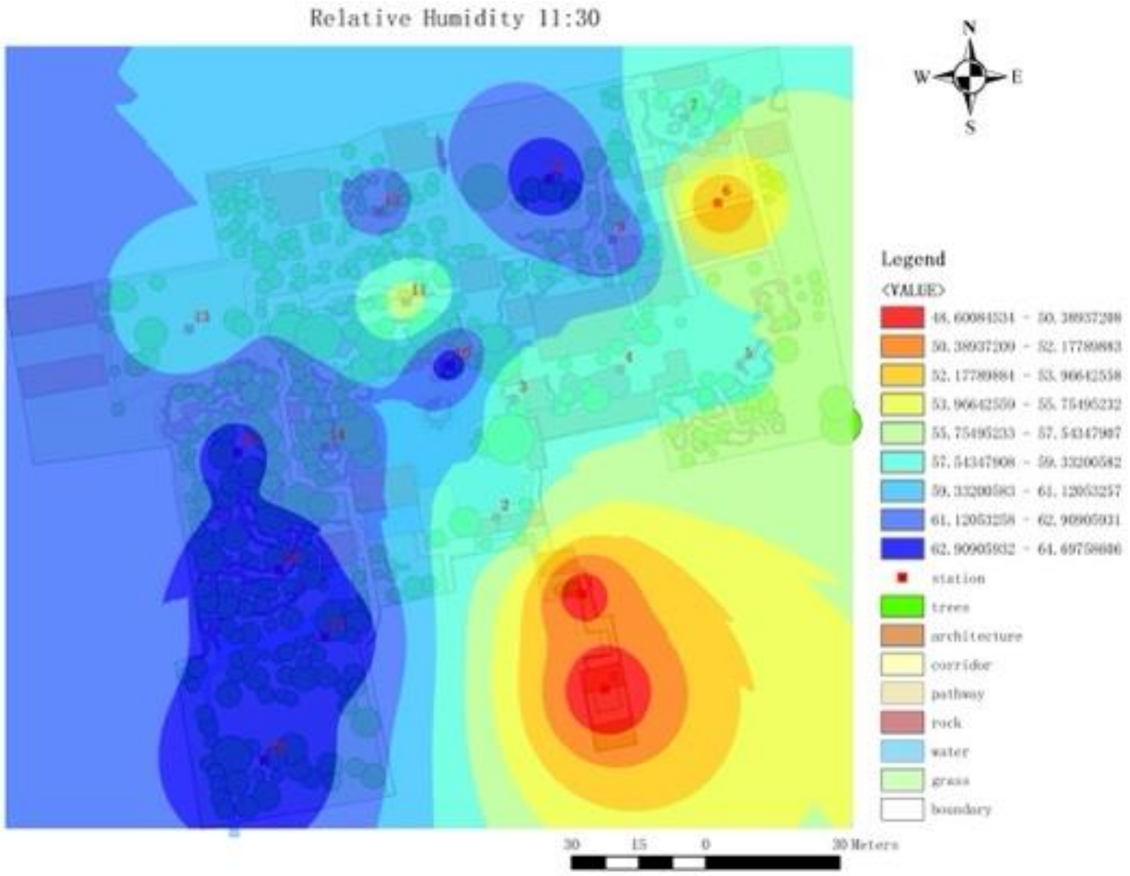
Relative Humidity 11:30
N
W
E
S
Legend
<VALUE>
48.60084534 - 50.38937208
50.38937209 - 52.17789883
52.17789884 - 53.96642558
53.96642559 - 55.75495232
55.75495233 - 57.54347907
57.54347908 - 59.33200582
59.33200583 - 61.12053257
61.12053258 - 62.90905931
62.90905932 - 64.69758606
station
trees
architecture
corridor
pathway
rock
water
grass
boundary
30
15
0
30 Meters

(c)

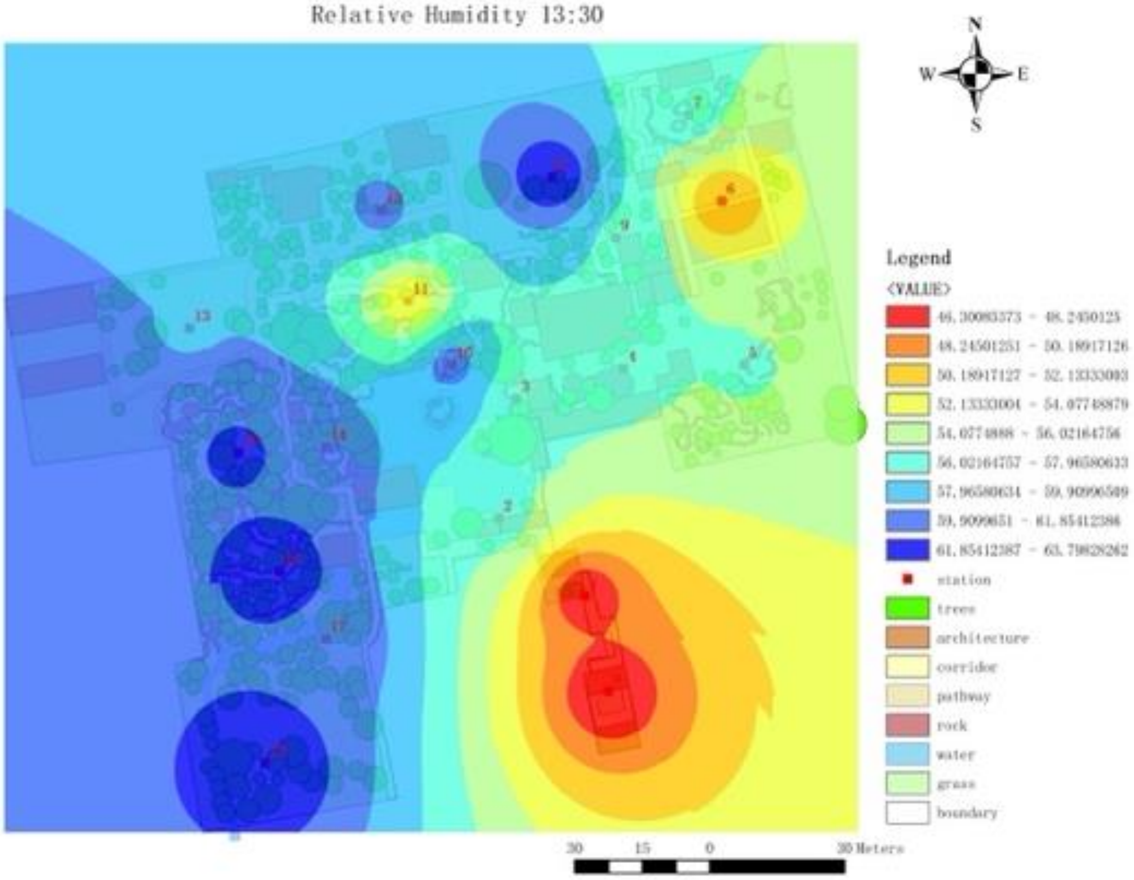
Relative Humidity 13:30
N
W
E
S
Legend
<VALUE>
46.30083373 - 48.2450125
48.24501251 - 50.18917126
50.18917127 - 52.13333003
52.13333004 - 54.07748879
54.0774888 - 56.02164756
56.02164757 - 57.96580633
57.96580634 - 59.90996509
59.9099651 - 61.85412386
61.85412387 - 63.79828262
station
trees
architecture
corridor
pathway
rock
water
grass
boundary
30
15
0
30 Meters

(d)

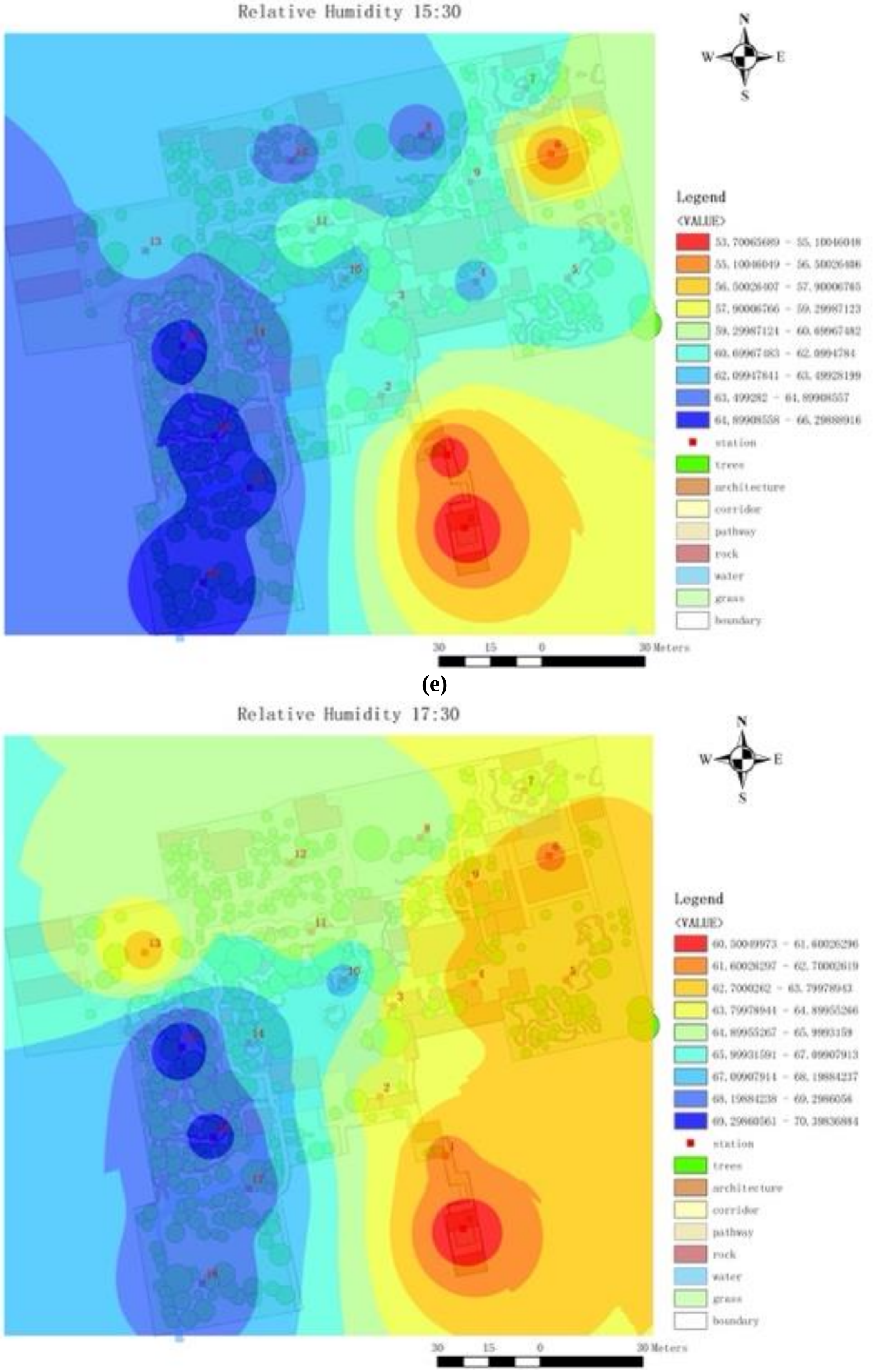

(e)

(f)

Figure 10. Relative humidity scenarios from 7:30 to 17:30 in the Lingering Garden.

Within the Lingering Garden, early morning humidity was consistently high in areas adjacent to vegetation and water, notably at station 18. Dense foliage and proximity to water bodies enhanced moisture retention, supporting higher humidity levels in these zones. Stations near the central pond, such as 11, showed moderate humidity levels due to the influence of open water. Areas with sparse vegetation and significant sunlight exposure, such as stations 0, 1, and 2, displayed lower humidity levels, as increased air circulation reduced ambient moisture. By midday, relative humidity decreased across the garden, especially in sunlit regions. Despite this trend, stations with substantial vegetation and water features, such as 16 and 18, maintained relatively high humidity due to continuous moisture release from these elements. In the late afternoon, as temperatures cooled, humidity levels began to rise, with vegetation and water bodies contributing to ambient moisture recovery.

The Canglang Pavilion demonstrated similar humidity dynamics, with values peaking in the morning (60–65%) around shaded areas with dense vegetation, notably stations 7, 3, and 8 (**Figure 11**). Locations near water bodies, such as stations 3 and 9, also displayed elevated humidity. As temperatures rose, humidity levels decreased, particularly in exposed areas like station 1, where relative humidity dropped to approximately 57%. The midday decline was most pronounced in sun-exposed zones, such as station 4, where relative humidity fell to between 50–55%. Nevertheless, areas near water and dense vegetation retained higher moisture levels. By late afternoon, as temperatures decreased, humidity levels gradually increased, particularly near shaded areas and water features.

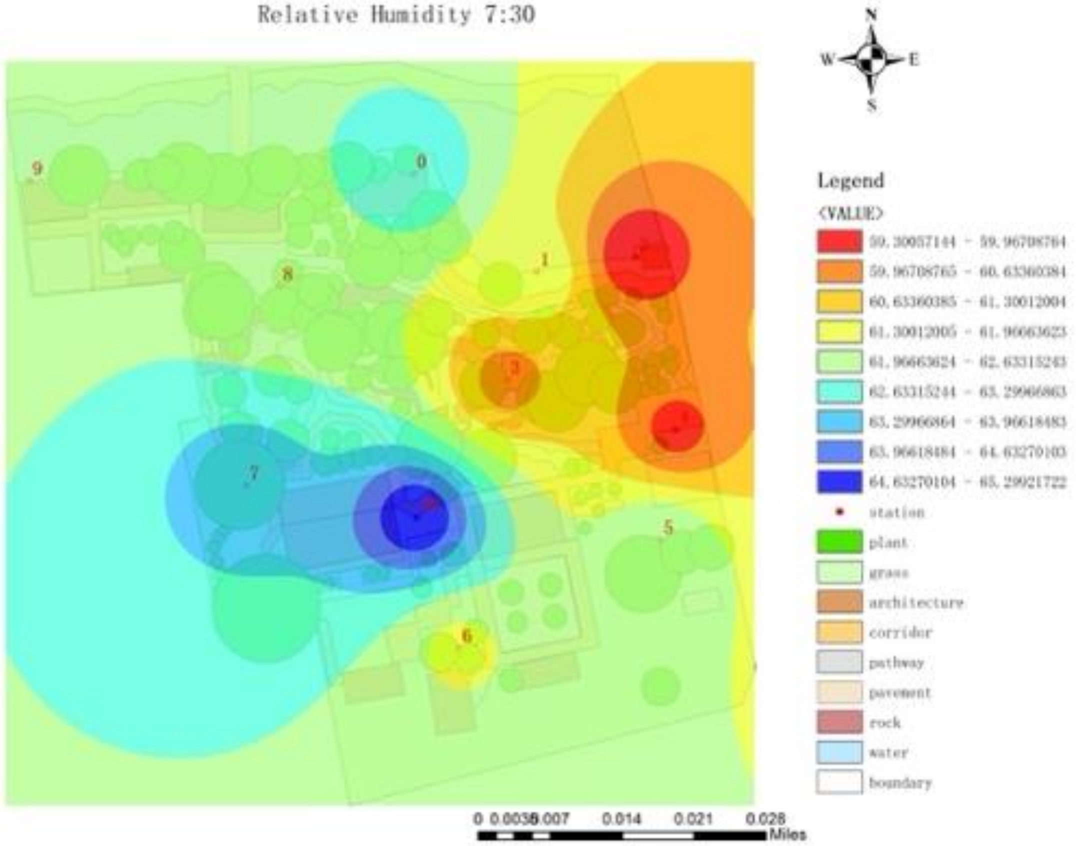

(a)

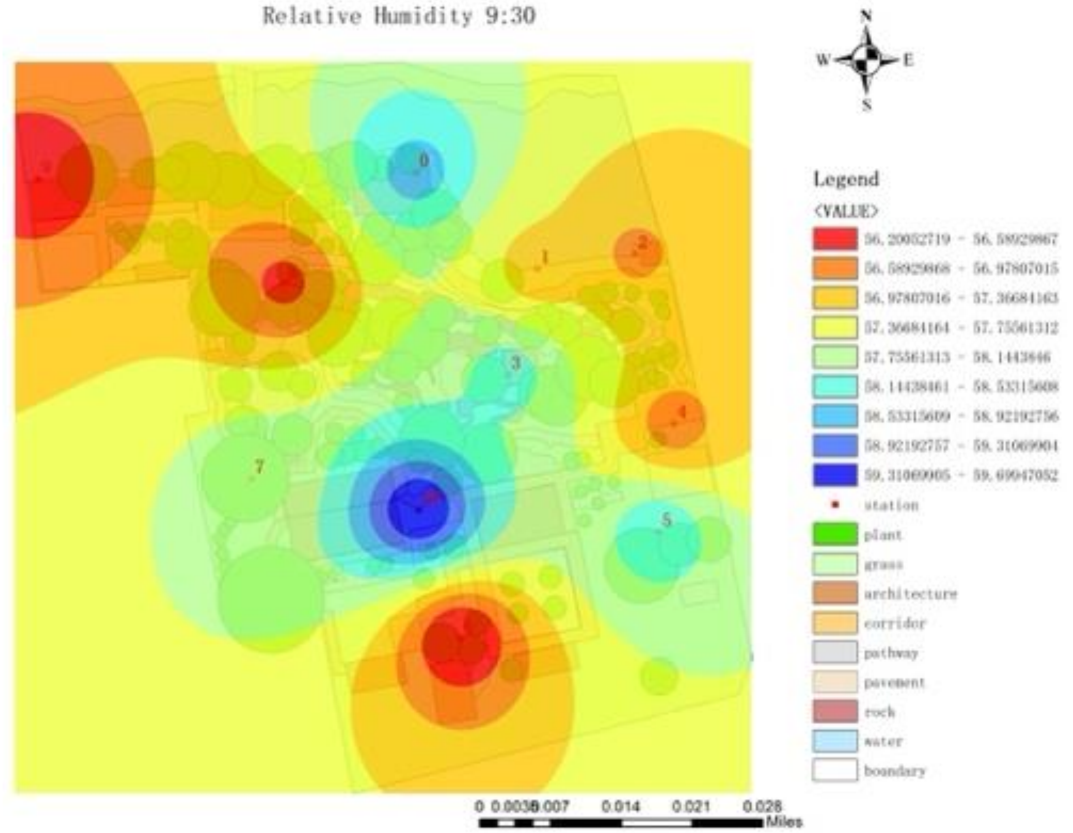
Relative Humidity 9:30
N
W
E
S
Legend
<VALUE>
56. 20052719 - 56. 58929867
56. 58929868 - 56. 97807015
56. 97807016 - 57. 36684163
57. 36684164 - 57. 75561312
57. 75561313 - 58. 1443846
58. 14438461 - 58. 53315608
58. 53315609 - 58. 92192756
58. 92192757 - 59. 31069904
59. 31069905 - 59. 69947052
station
plant
grass
architecture
corridor
pathway
pavement
rock
water
boundary
0
1
2
3
4
5
7
0 0.0035 0.007 0.014 0.021 0.028
Miles

(b)

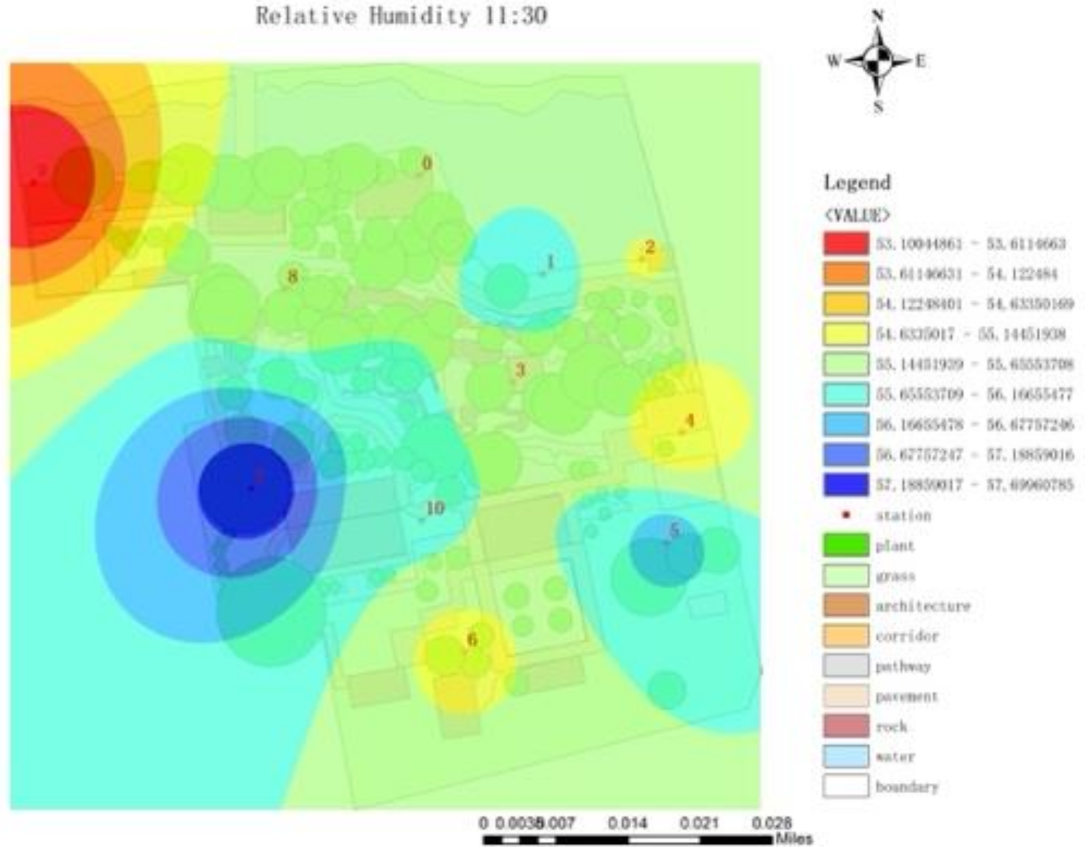
Relative Humidity 11:30
N
W
E
S
Legend
<VALUE>
53. 10044861 - 53. 6114663
53. 61146631 - 54. 122484
54. 12248401 - 54. 63350169
54. 6335017 - 55. 14451938
55. 14451939 - 55. 65553708
55. 65553709 - 56. 16655477
56. 16655478 - 56. 67757246
56. 67757247 - 57. 18859016
57. 18859017 - 57. 69960785
station
plant
grass
architecture
corridor
pathway
pavement
rock
water
boundary
0
1
2
3
4
5
6
8
10
0 0.0035 0.007 0.014 0.021 0.028
Miles

(c)

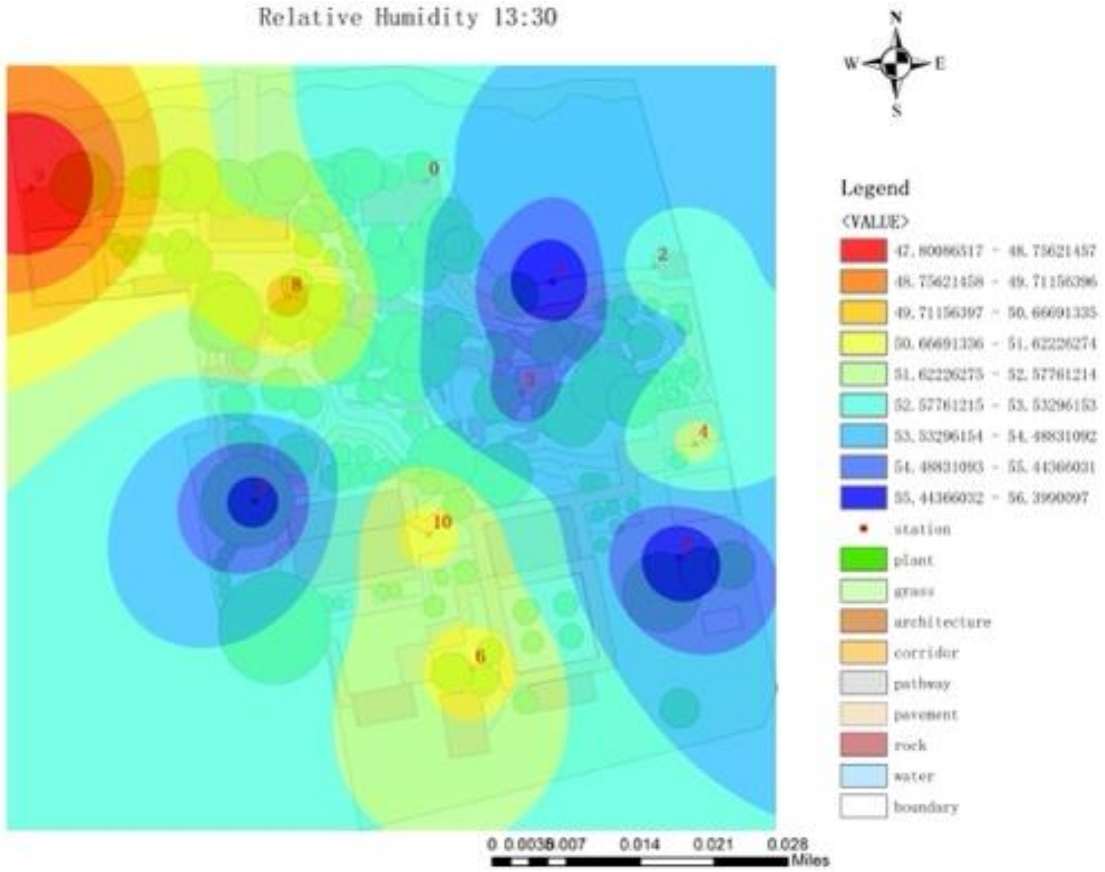
Relative Humidity 13:30
N
W
E
S
Legend
<VALUE>
🟥 47.80086517 - 48.75621457
🟧 48.75621458 - 49.71156396
🟨 49.71156397 - 50.66691335
🟨 50.66691336 - 51.62226274
🟩 51.62226275 - 52.57761214
🟦 52.57761215 - 53.53296153
🟦 53.53296154 - 54.48831092
🟦 54.48831093 - 55.44366031
🟦 55.44366032 - 56.3990097
● station
🟩 plant
🟩 grass
🟫 architecture
🟧 corridor
⬜ pathway
⬜ pavement
🟥 rock
🟦 water
⬜ boundary
0
2
4
8
10
6
0 0.0035 0.007 0.014 0.021 0.028
Miles

(d)

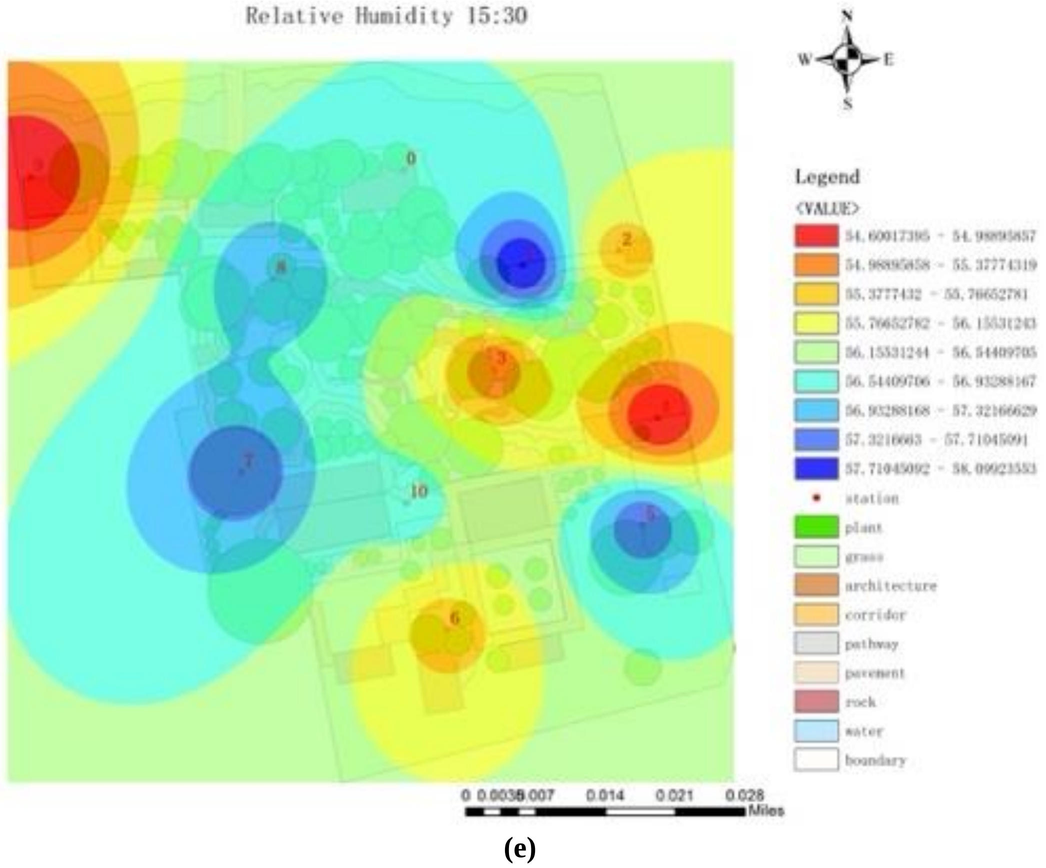
Relative Humidity 15:30
N
W
E
S
Legend
<VALUE>
🟥 54.60017395 - 54.98895857
🟧 54.98895858 - 55.37774319
🟨 55.3777432 - 55.76652781
🟨 55.76652782 - 56.15531243
🟩 56.15531244 - 56.54409705
🟦 56.54409706 - 56.93288167
🟦 56.93288168 - 57.32166629
🟦 57.3216663 - 57.71045091
🟦 57.71045092 - 58.09923553
● station
🟩 plant
🟩 grass
🟫 architecture
🟧 corridor
⬜ pathway
⬜ pavement
🟥 rock
🟦 water
⬜ boundary
0
2
8
3
7
10
5
6
0 0.0035 0.007 0.014 0.021 0.028
Miles

(e)

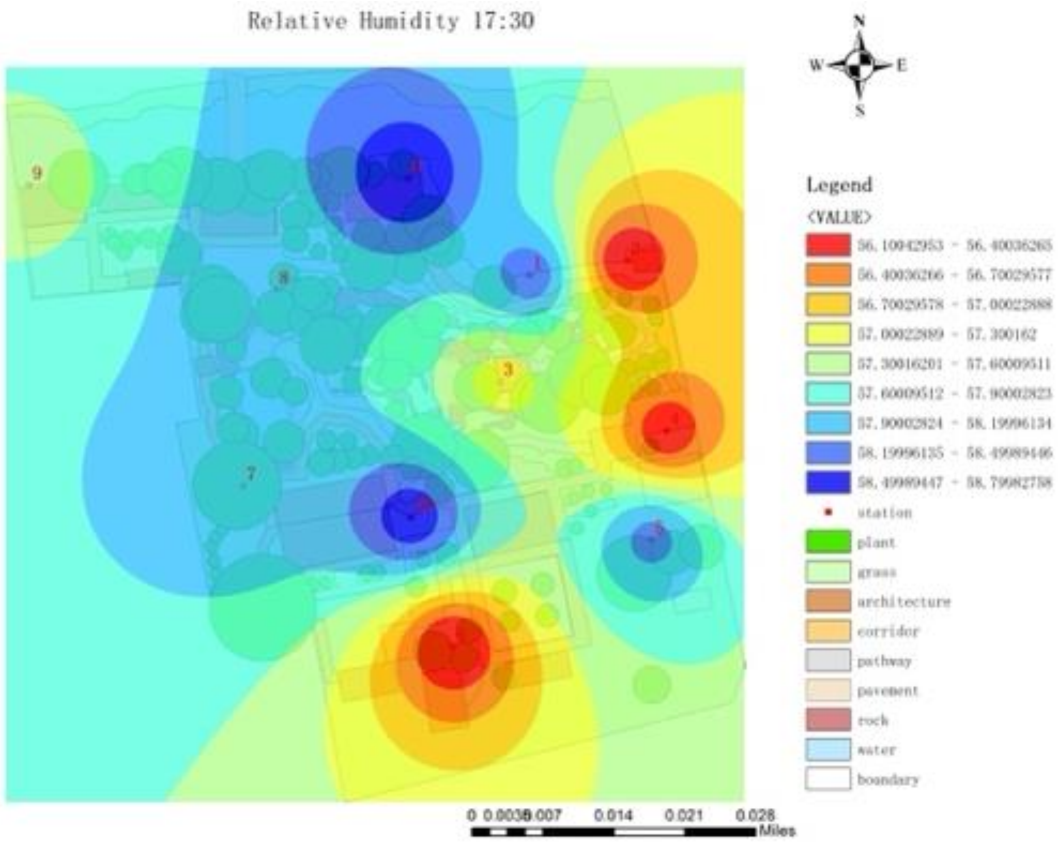

(f)

Figure 11. Relative humidity scenarios from 7:30 to 17:30 in the Canglang Pavilion.

In summary, these three gardens had consistently higher humidity levels in the morning near water bodies and dense vegetation. This was attributed to the moisture retention capacity of the vegetation and the evaporative cooling effect of the water bodies. As the day progressed, humidity levels decreased, especially in sunny and less vegetated areas. These findings emphasize the importance of water bodies and vegetation in maintaining humidity levels in gardens, contributing to a more comfortable microclimate.

5. Discussion

The spatial interpolation analysis of microclimate data demonstrates the intricate interplay between landscape elements and microclimatic modulation within Classical Chinese Gardens. These findings underscore the effectiveness of traditional garden designs in managing air temperature and relative humidity, which are essential for creating comfortable outdoor environments.

5.1. Temperature and humidity modulation through landscape design

The IDW analysis revealed that water bodies and dense vegetation are critical in regulating air temperature and relative humidity across all three gardens. The Humble Administrator’s Garden, with its extensive water features and layered vegetation, exhibited the most effective cooling capability, with temperature reductions noted near water bodies (stations 12 and 16). Similarly, areas with dense vegetation showed lower temperature readings and stable humidity, highlighting the synergy between evapotranspiration from vegetation and evaporative cooling from water bodies. In the Lingering Garden, water and vegetation also significantly impacted microclimate regulation. However, the interplay with architectural elements created distinct thermal zones. Stations near dense vegetation and water, such as stations 16 and 18, maintained lower temperatures and higher humidity, while areas with hardscape elements retained heat longer into the evening, indicating the heat retention properties of rockeries and built structures. This contrast demonstrates how the juxtaposition of natural and architectural elements in Classical Chinese Gardens can create varied thermal experiences within a single garden space.

The IDW results for Lingering Garden specifically highlighted the role of rockeries and architectural elements in microclimatic regulation. Stations near rockeries and pathways recorded higher midday temperatures due to thermal mass and heat retention. However, shaded spaces created by the positioning of these elements also provided relief from direct sunlight, enabling nuanced thermal modulation. This suggests that strategic placement of hardscape features, when combined with vegetative cover, can control temperature variation effectively.

The Canglang Pavilion demonstrated that even smaller gardens can achieve significant microclimatic benefits through dense vegetation and water proximity. Stations near water and trees (stations 3 and 7) showed lower temperature readings and stable humidity, even during midday. The compact arrangement of these features ensured rapid temperature recovery in the evening, as dense vegetation and water facilitated cooling through retained moisture. The Canglang Pavilion's design illustrates how smaller-scale green spaces can leverage vegetation density and water to achieve efficient thermal regulation.

5.2. Implication for urban park design

The findings from this study's IDW spatial interpolation analysis of Classical Chinese Gardens (CCGs) provide significant insights for enhancing urban park design, especially in the context of sustainable climate adaptation strategies. Integrating traditional garden elements—such as water bodies, layered vegetation, and hardscape features—can enable modern urban parks to mitigate urban heat island (UHI) effects, enhance thermal comfort, and promote environmental resilience. The following design recommendations, inspired by the landscape configurations of the Humble Administrator's Garden, Lingering Garden, and Canglang Pavilion, suggest specific strategies for creating microclimatically favorable urban green spaces.

Water bodies were found to have consistent cooling effects across all three CCGs studied, significantly lowering air temperatures and stabilizing relative humidity in surrounding areas. For urban parks, incorporating ponds, fountains, or artificial streams can similarly serve as natural cooling agents. Placing water features in areas with high foot traffic or where thermal relief is most needed can create cooling zones within densely built environments, thereby helping to alleviate the UHI effect. Additionally, situating water bodies adjacent to vegetation can amplify cooling through the combined effects of evapotranspiration and evaporative cooling, offering more localized and effective thermal comfort. The layered vegetation characteristic of

CCGs, including canopies, mid-height shrubs, and ground cover, was shown to reduce temperatures through shading and humidity retention. This multi-layered approach is recommended for urban park designs, where tall trees forming a canopy layer can intercept sunlight while understory shrubs and ground vegetation further insulate the soil and promote humidity. Such vegetation layering provides a cooling buffer during peak midday hours and supports a more varied ecosystem. Selecting native species with high transpiration rates can further enhance the cooling effects, while layered vegetation encourages biodiversity by providing habitats for urban wildlife, thus contributing to a healthier ecosystem.

The Lingering Garden’s interplay between rockeries and vegetative shade demonstrates the potential of hardscape elements in modulating microclimate when used judiciously. In urban parks, shaded seating, pathways, and architectural structures can provide temperature variation and support user comfort. Hardscape materials should be positioned strategically, where they receive partial shade to reduce midday heat buildup, and designed with materials that retain less heat, such as lighter or porous stones. This strategy allows urban parks to provide cooler spaces for rest and recreation while managing the heat absorption of hardscape materials. The Canglang Pavilion exemplifies the capacity of compact gardens to achieve significant cooling and humidity retention through dense planting and water features. For urban settings with limited available land, the compact design approach used in CCGs can inspire the creation of small, multifunctional parks or pocket parks. Dense vegetation and water bodies within confined areas provide concentrated cooling benefits, effectively turning small green spaces into neighborhood cooling zones. This approach not only makes efficient use of limited space but also ensures that each section of the park contributes to overall thermal regulation and comfort, serving as an inviting oasis for nearby residents.

5.3. Limitations and future research

This study provides valuable insights into the microclimatic effects of landscape elements in Classical Chinese Gardens (CCGs) through IDW spatial interpolation, yet several limitations should be acknowledged. Firstly, the analysis is constrained by temporal and seasonal data coverage, as data were only collected during a specific summer period. Consequently, microclimatic variations across different seasons, particularly during colder months, were not assessed. Future research could benefit from multi-seasonal data collection to capture the full spectrum of microclimatic behavior within these gardens. Secondly, while the IDW interpolation method offers a useful tool for spatial analysis, it is inherently limited in its assumptions about spatial homogeneity and may not fully capture complex, non-linear microclimatic interactions among landscape elements. Incorporating more advanced interpolation methods, such as kriging or machine-learning-based spatial modeling, could improve accuracy by accounting for non-linear and site-specific microclimatic influences.

6. Conclusion

By analyzing the microclimates of Suzhou’s Humble Administrator’s Garden, Lingering Garden, and Canglang Pavilion in detail, this study reveals the synergistic effects of water bodies, vegetative cover, and hardscape elements in creating a comfortable environment. Together, these elements significantly reduced air temperature and maintained relatively stable humidity levels. Specifically, water bodies demonstrated a sustained cooling effect in all three gardens, significantly lowering air temperatures and stabilizing relative humidity in the surrounding areas. Vegetation, especially the multi-layered vegetation configuration, provided additional cooling effects through transpiration while promoting increased biodiversity. In addition, the proper placement of hardscape elements, such as the use of rocks and buildings to generate shade spaces, moderates the microclimate to some extent. Although these spaces are easily overlooked, they are critical to improving urban resilience and the well-being of residents. To translate these findings into practical action, we propose the following constructive approaches and strategies.

First, when designing urban green spaces, urban planners should prioritize the addition of water bodies and vegetation cover to improve the cooling effect of green spaces. In addition, the layout of green spaces should be integrated with urban airways to promote the dispersion of hot air and the circulation of cool air. Secondly, for small-scale spaces such as pocket parks, multi-layered vegetation configurations, the use of permeable paving materials, and the incorporation of small bodies of water should be emphasized to enhance their microclimate regulation. In addition, to mitigate the UHI effect, it is recommended that more green spaces and water bodies be installed in urban heat island hotspots, as well as green roofs and wall greening be promoted to increase the reflectivity of urban surfaces to solar radiation. Finally, to reduce surface runoff, it is recommended that rain gardens and permeable paving be incorporated into the design of urban green spaces to promote rainwater infiltration and retention, reduce runoff and enhance groundwater recharge. Future research should further explore the specific implementation effects of these strategies and continuously optimize and adjust them based on empirical data.

In summary, the findings of this study not only deepen our understanding of the role of classical garden design principles in climate adaptation, but also provide valuable theoretical support for sustainable urban design. Especially in the context of global urbanization and climate change, the application of these traditional design principles is important for mitigating the urban heat island effect, enhancing the thermal comfort of urban residents, and increasing the resilience of urban environments. In addition, the application of GIS technology in visualizing and optimizing the urban microclimate provides new theoretical tools and methods in the field of urban planning and environmental management, which helps to better understand and imitate the microclimate regulation mechanism in natural ecosystems, provides a scientific basis for the design of urban greening and parks, and promotes the sustainable development of urban environments.

Conflict of interest: The authors declare no conflict of interest.

References

Back, Y et al. (2022). Integrating CFD-GIS modelling to refine urban heat and thermal comfort assessment. Science of the Total Environment. https://doi.org/10.1016/j.scitotenv.2022.159729

Chen, X., & Li, Y. (2020). Harmonizing nature and architecture: A study of Suzhou’s classical gardens. Journal of Landscape and Urban Planning, 98(4), pp.456–472.

Fang, Z., & Chen, L. (2019). Microclimate performance of Suzhou gardens: A case study of Canglang Pavilion. Journal of Environmental Studies, 32(3), pp.123–134.

Guerri, G., Crisci, A., & Morabito, M. (2023). Urban microclimate simulations based on GIS data to mitigate thermal hot-spots: Tree design scenarios in an industrial area of Florence. Building and Environment, 110854, pp.245. https://doi.org/10.1016/j.buildenv.2023.110854

Guo et al. (2022). The influence of landscape design parameters on the summer microclimate and thermal comfort of Suzhou classical gardens. Journal of Chinese Urban Forestry, 20(1), pp.49–55.

Henderson, J. V., & Turner, M. A. (2020). Urbanization in the Developing World: Too Early or Too Slow? Journal of Economic Perspectives, 34(3), pp.150–173. https://doi.org/10.1257/jep.34.3.150

Huang et al. (2011). Explorations of the implementation of a parallel IDW interpolation algorithm in a Linux cluster-based parallel GIS. Computers and Geosciences, 37(4), pp.426–434. https://doi.org/10.1016/j.cageo.2010.05.024

Liu, J., Wang, S., & Zhao, T. (2020). Thermal performance and design principles of Lingering Garden. Urban Climate, 100687, pp.35.

Mangiameli, M., Mussumeci, G., & Gagliano, A. (2022). Evaluation of the Urban Microclimate in Catania Using Multispectral Remote Sensing and GIS Technology. Climate, 10(2), Article 2. https://doi.org/10.3390/cli10020018

Nazarian et al. (2017). Predicting outdoor thermal comfort in urban environments: A 3D numerical model for standard effective temperature. Urban Climate, 20, pp.251–267. https://doi.org/10.1016/j.uclim.2017.04.011

Nusret, D., & Dug, S. (2012). Applying The Inverse Distance Weighting And Kriging Methods Of The Spatial Interpolation On The Mapping The Annual Precipitation In Bosnia And Herzegovina (Vol. 12, pp. 0). https://scholarsarchive.byu.edu/iemssconference/2012/Stream-B/229

Peng et al. (2019). Spatial-temporal pattern of, and driving forces for, urban heat island in China. Ecological Indicators, 96, pp.127–132. https://doi.org/10.1016/j.ecolind.2018.08.059

Ren et al. (2022). Rapid urbanization and climate change significantly contribute to worsening urban human thermal comfort: A national 183-city, 26-year study in China. Urban Climate, 101154, pp.43. https://doi.org/10.1016/j.uclim.2022.101154

Santamouris, M. (2015). Analyzing the heat island magnitude and characteristics in one hundred Asian and Australian cities and regions. Science of The Total Environment, pp.512–513, 582–598. https://doi.org/10.1016/j.scitotenv.2015.01.060

Sun et al. (2020). Dramatic uneven urbanization of large cities throughout the world in recent decades. Nature Communications, 11(1), pp.5366. https://doi.org/10.1038/s41467-020-19158-1

Wang, R., & Zhang, P. (2019). Architectural sequences in Lingering Garden: Enhancing microclimatic comfort. Landscape Journal, 45(2), pp.201–214.

Xiong et al. (2020). Strategies for improving the microclimate and thermal comfort of a classical Chinese garden in the hot-summer and cold-winter zone. Energy & Buildings, 109914, pp.215. https://doi.org/10.1016/j.enbuild.2020.109914

Xu, L., Zhang, F., & Zhou, H. (2018). Historical significance and environmental benefits of Suzhou’s classical gardens. Environmental Research, 27(5), pp.112–124.

Yu et al. (2020). Critical review on the cooling effect of urban blue-green space: A threshold-size perspective. https://doi.org/10.1016/j.ufug.2020.126630

Zhou, Y., Wu, Q., & Li, K. (2021). Cooling effects of water and vegetation in Humble Administrator’s Garden. Journal of Urban Ecology, 29(6), pp.987–996.